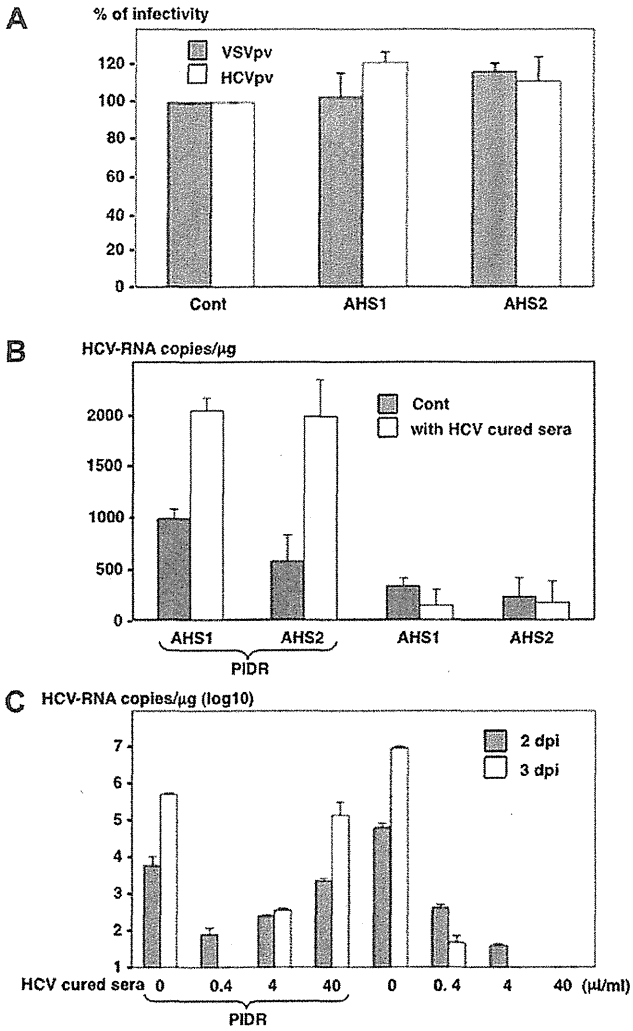

Fig. 4. Neutralizing antibodies in the CHS enhanced the PIDR-mediated entry of HCV. (A) The absence of neutralizing antibodies in the sera from acute hepatitis C patients (AHS) was determined by a neutralization assay using the HCVpv (white bars) and VSVpv (gray bar). (B) The effect of PIDR on the entry of HCVser into Huh7OK1 cells in the presence of neutralizing antibodies. The AHS were incubated with the CHS carrying neutralization antibodies but no infectious HCV obtained from patients cured by the IFN therapy (white bars) or HDS (gray bar) in the presence (left) or absence (right) of PIDR and inoculated into Huh7OK1 cells. The HCV-RNA titers in cells were determined at 24 h post-inoculation. (C). The effect of neutralizing antibodies on the PIDR-mediated infection of HCVcc. Huh7OK1 cells were inoculated with HCVcc at an MOI of 0.05 after incubation with 0.4–40 μl/ml of HCV-negative CHS in the presence (left) or absence (right) of PIDR. Gray and white bars indicate the HCV-RNA titers at 2 and 3 days after infection, respectively.

3.7. Effect of PIDR on the entry of HCVser into immortalized human hepatocytes

Recently, Aly et al. reported that immortalized human hepatocytes, HuS/E2 cells, exhibited a high susceptibility to the infection with HCVser [7]. Therefore, we examined the effect of PIDR on the entry of HCVser into immortalized human hepatocytes, including Hc and HuS/E2 cells. The addition of PIDR enhanced the entry of HCVser into both Hc and HuS/E2 cells

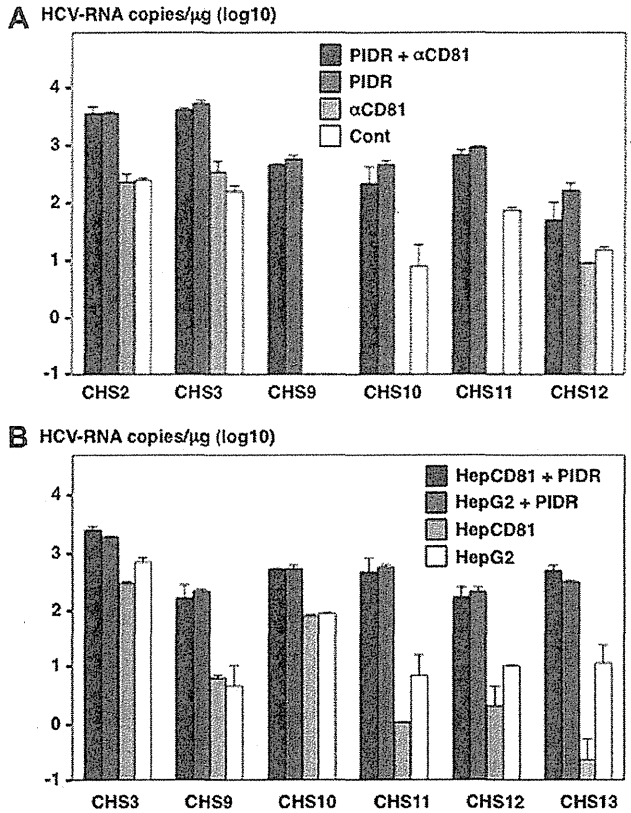

Fig. 5. Human CD81-independent entry of HCVser by PIDR. (A) The effect of anti-hCD81 antibody on the entry of HCVser into Huh7OK1 cells in the presence or absence of PIDR. (B) The effect of PIDR on the entry of HCVser into HepG2 and HepCD81 cells. HCV-RNA titers in cells were determined at 24 h post-inoculation.

(Fig. 6A and B). These results indicate that PIDR has the potential to enhance the entry of HCVser into not only cancer cell lines but also immortalized hepatocytes. Next, to evaluate the long-term effect of PIDR treatment on the infectivity of HCVser, Hc cells inoculated with CHS pre-incubated with PIDR were cultured for a long period. HCV-RNA could be detected at 10, 15 and 20 days after PIDR-mediated infection (Fig. 6C). However, significant elevations of HCV-RNA titers were not seen (Data not shown).

4. Discussion

In this study, we examined the efficiency of intracellular deliveries of HCVser by using spinoculation, polybrene and PIDR and found that the PIDR exhibited the highest efficacy on the entry of HCVser into target cells. Especially, trypsinization and reseeding of cells dramatically reduced HCV-RNA levels in groups that were not treated with PIDR as compared to those were treated with PIDR (Fig. 3B and C), and PIDR treatment dramatically increased the internalization of HCVcc treated with CHS or AP-33 at 2 and 4 days after infection (Fig. 2B and C). These results suggest that PIDR is feasible to deliver HCV/CHS complexes into target cells that allow productive infection. In addition, PIDR facilitated the entry of

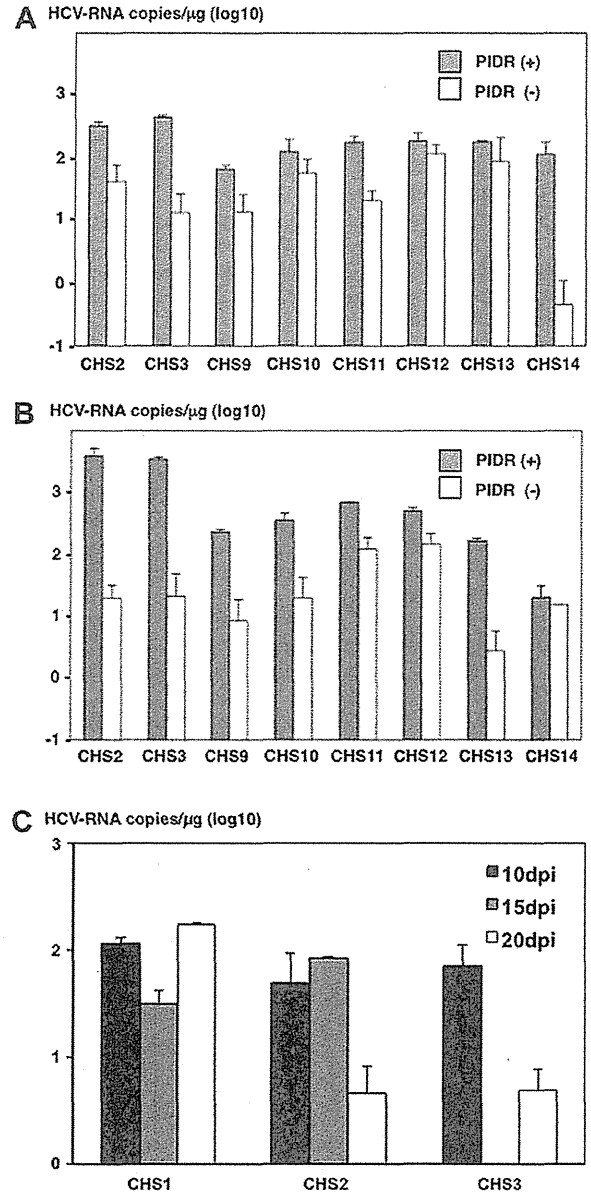

Fig. 6. Effect of PIDR on the entry of HCVser into immortalized human hepatocytes. The effect of PIDR on the entry of HCVser into immortalized human hepatocytes, such as Hc (A) and HuS/E2 (B) cells. The HCV-RNA titers in cells were determined at 24 h post-inoculation. (C) HCV-RNA titers in Hc cells inoculated with HCVser were evaluated at 10, 15 and 20 days after PIDR-mediated infection.

HCVser into the hepatoma cell lines and immortalized human hepatocytes in an hCD81-independent manner. Furthermore, we demonstrated that the intracellular delivery of HCVser by PIDR was enhanced by the addition of anti-HCV antibodies in sera from chronic hepatitis C patients, suggesting that PIDR is an effective reagent for the intracellular delivery of HCVser into the target cells in a receptor-independent manner.

Although direct evidence of enhancement of the adsorption and penetration by the application of spinoculation and polybrene has not been demonstrated yet, sedimentation of the virus particles to the cell surface by the spinoculation and electrostatic interactions between viral particles and cells by the charged polybrene are suggested to overcome the first barrier between virus particles and cells [12–14]. PIDR is a cationic amphiphilic-based protein delivery reagent that forms a complex with proteins through electrostatic and hydrophobic interactions [17]. The complexes of protein molecules and PIDR have been shown to interact with heparan sulfate proteoglycans on the cell surface, and then to be internalized through endocytosis, after which the protein molecules are released from the complexes into the cytoplasm [17], suggesting that PIDR is capable of enhancing not only adsorption but also penetration of HCVser.

Although HCVser are composed of heterogenous viral populations and a large fraction of the viral particles was associated with lipoproteins or neutralizing antibodies [25], these particles are capable of invading into human hepatocytes and establishing a persistent infection *in vivo* [1]. Therefore, it is feasible to speculate that some host factors are involved in the entry of HCVser into hepatocytes *in vivo*. Recently, Stamataki et al. [26] suggested that peripheral blood B lymphocytes participate as a reservoir for HCV for persistent infection and as a vehicle for transinfection to hepatocytes. Although the precise mechanisms of the entry of HCV have not been clarified yet, PIDR is an efficient modality to overcome the obstacles to the entry of HCV.

Recent studies have revealed that at least four cellular molecules play crucial roles in the infection of HCV into hepatocytes *in vitro*: hCD81, scavenger receptor class B type I (SR-BI) [27], and tight junction proteins claudin-1 [28] and occludin [11]. In this study, the entry of HCVser by the treatment with PIDR was shown to be independent from hCD81. Although the involvement of receptor candidates other than hCD81 was not examined in this study, PIDR was shown to enhance the entry of HCVser in cell lines including Huh7, HepG2, HepCD81, Hc and HuS/E2, suggesting that PIDR is capable of enhancing the entry of HCV through a pathway independent from the expression of these receptor candidates.

Previous studies have indicated that HCV infects not only hepatocytes but also lymphoid tissues and peripheral blood mononuclear cells [29], and that the quasispecies nature of viral particles was different among tissues infected with HCV [10]. Furthermore, it was shown that the *in vitro* transcribed JFH-1 RNA used for the recovery of infectious particles contained 2.21×10^{11} copies/μg [30], which is much higher than the amount of viral RNA detected in the patient's sera. The variety of cell tropisms depending on the quasispecies of HCV particles, a low viral load in sera co-existing with neutralization antibodies, and the lack of identified co-factors including functional environment of the liver might be the major obstacles to establishing cell culture systems for the propagation of HCVser. Several approaches have been taken for the establishment of an *in vitro* cell culture system of HCV, including the culture of human liver cells in a three-dimensional radial-flow bioreactor [31], the three-dimensional culture of immortalized primary hepatocytes [7], and the micropatterned culture of primary hepatocytes [8]. These innovative approaches to the cell culture of liver cells, in combination with PIDR which is able to overcome the first barrier of HCV propagation might

contribute to a breakthrough in the establishment of a robust cell culture system of HCVser.

In this study, we demonstrated that PIDR is able to internalize HCV in a receptor-independent manner and provides a clue toward the development of a cell culture system of HCVser in the presence of neutralization antibodies. PIDR may also be useful for the study of viruses that are difficult to internalize into cells due to their low viral titers or the presence of neutralizing antibodies.

Acknowledgments

We thank H. Murase for secretarial work.

This research was supported in part by grants-in-aid from the Ministry of Health, Labor, and Welfare, and the Ministry of Education, Culture, Sports, Science, and Technology, Japan.

References

[1] L.-B. Seeff, Natural history of chronic hepatitis C, Hepatology 36 (2002) S35–S46.

[2] M.-P. Manns, J.-G. McHutchison, S.-C. Gordon, V.-K. Rustgi, M. Shiffman, R. Reindollar, Z.-D. Goodman, K. Koury, M. Ling, J.-K. Albrecht, Peginterferon alfa-2b plus ribavirin compared with interferon alfa-2b plus ribavirin for initial treatment of chronic hepatitis C: a randomised trial, Lancet 358 (2001) 958–965.

[3] J.-M. Pawlotsky, S. Chevaliez, J.-G. McHutchison, The hepatitis C virus life cycle as a target for new antiviral therapies, Gastroenterology 132 (2007) 1979–1998.

[4] T. Wakita, T. Pietschmann, T. Kato, T. Date, M. Miyamoto, Z. Zhao, K. Murthy, A. Habermann, H.-G. Krausslich, M. Mizokami, R. Bartenschlager, T. Jake-Liang, Production of infectious hepatitis C virus in tissue culture from a cloned viral genome, Nat. Med. 11 (2005) 791–796.

[5] N. Hiraga, M. Imamura, M. Tsuge, C. Noguchi, S. Takahashi, E. Iwao, Y. Fujimoto, H. Abe, T. Maekawa, H. Ochi, C. Tateno, K. Yoshizawa, A. Sakai, Y. Sakai, M. Honda, S. Kaneko, T. Wakita, K. Chayama, Infection of human hepatocyte chimeric mouse with genetically engineered hepatitis C virus and its susceptibility to interferon, FEBS Lett. 581 (2007) 1983–1987.

[6] S. Molina, V. Castet, L. Pichard-Garcia, C. Wychowski, E. Meurs, J.-M. Pascussi, C. Sureau, J.-M. Fabre, A. SaCunha, D. Larrey, J. Dubuisson, J. Coste, J. McKeating, P. Maurel, C. Fournier-Wirth, Serum-derived hepatitis C virus infection of primary human hepatocytes is tetraspanin CD81 dependent, J. Virol. 82 (2008) 569–574.

[7] H.-H. Aly, Y. Qi, K. Atsuzawa, N. Usuda, Y. Takada, M. Mizokami, K. Shimotohno, M. Hijikata, Strain-dependent viral dynamics and virus-cell interactions in a novel in vitro system supporting the life cycle of blood-borne hepatitis C virus, Hepatology 50 (2009) 689–696.

[8] A. Ploss, S.-R. Khetani, C.-T. Jones, A.-J. Syder, K. Trehan, V.-A. Gaysinskaya, K. Mu, K. Ritola, C.-M. Rice, S.-N. Bhatia, Persistent hepatitis C virus infection in microscale primary human hepatocyte cultures, Proc. Natl. Acad. Sci. U. S. A 107 (2010) 3141–3145.

[9] D.-R. Burton, Antibodies, viruses and vaccines, Nat. Rev. Immunol. 2 (2002) 706–713.

[10] R. Sobesky, C. Feray, F. Rimlinger, N. Derian, A. Dos Santos, A.-M. Roque-Afonso, D. Samuel, C. Brechot, V. Thiers, Distinct hepatitis C virus core and F protein quasispecies in tumoral and nontumoral hepatocytes isolated via microdissection, Hepatology 46 (2007) 1704–1712.

[11] A. Ploss, M.-J. Evans, V.-A. Gaysinskaya, M. Panis, H. You, Y.-P. de Jong, C.-M. Rice, Human occludin is a hepatitis C virus entry factor required for infection of mouse cells, Nature 457 (2009) 882–886.

[12] N. Landazuri, J.-M. Le Doux, Complexation of retroviruses with charged polymers enhances gene transfer by increasing the rate that viruses are delivered to cells, J. Gene Med. 6 (2004) 1304–1319.

[13] U. O'Doherty, W.-J. Swiggard, M.-H. Malim, Human immunodeficiency virus type 1 spinoculation enhances infection through virus binding, J. Virol. 74 (2000) 10074–10080.

[14] R. Watanabe, S. Matsuyama, F. Taguchi, Receptor-independent infection of murine coronavirus: analysis by spinoculation, J. Virol. 80 (2006) 4901–4908.

[15] L. Ye, X. Wang, S. Wang, G. Luo, Y. Wang, H. Liang, W. Ho, Centrifugal enhancement of hepatitis C virus infection of human hepatocytes, J. Virol. Methods 148 (2008) 161–165.

[16] I. Benedicto, F. Molina-Jimenez, B. Bartosch, F.-L. Cosset, D. Lavillette, J. Prieto, R. Moreno-Otero, A. Valenzuela-Fernandez, R. Aldabe, M. Lopez-Cabrera, The tight junction-associated protein occludin is required for a postbinding step in hepatitis C virus entry and infection, J. Virol. 83 (2009) 8012–8020.

[17] C.-O. Weill, S. Biri, A. Adib, P. Erbacher, A practical approach for intracellular protein delivery, Cytotechnology 56 (2008) 41–48.

[18] T. Okamoto, H. Omori, Y. Kaname, T. Abe, Y. Nishimura, T. Suzuki, T. Miyamura, T. Yoshimori, K. Moriishi, Y. Matsuura, A single-amino-acid mutation in hepatitis C virus NS5A disrupting FKBP8 interaction impairs viral replication, J. Virol. 82 (2008) 3480–3489.

[19] H. Tani, Y. Komoda, E. Matsuo, K. Suzuki, I. Hamamoto, T. Yamashita, K. Moriishi, K. Fujiyama, T. Kanto, N. Hayashi, A. Owsianka, A.-H. Patel, M.-H. Whitt, Y. Matsuura, Replication-competent recombinant vesicular stomatitis virus encoding hepatitis C virus envelope proteins, J. Virol. 81 (2007) 8601–8612.

[20] H.-H. Aly, K. Watashi, M. Hijikata, H. Kaneko, Y. Takada, H. Egawa, S. Uemoto, K. Shimotohno, Serum-derived hepatitis C virus infectivity in interferon regulatory factor-7-suppressed human primary hepatocytes, J. Hepatol. 46 (2007) 26–36.

[21] J. Zhong, P. Gastaminza, G. Cheng, S. Kapadia, T. Kato, D.-R. Burton, S.-F. Wieland, S.-L. Uprichard, T. Wakita, F.-V. Chisari, Robust hepatitis C virus infection in vitro, Proc. Natl. Acad. Sci. U. S. A 102 (2005) 9294–9299.

[22] T. Morris, B. Robertson, M. Gallagher, Rapid reverse transcription-PCR detection of hepatitis C virus RNA in serum by using the TaqMan fluorogenic detection system, J. Clin. Microbiol. 34 (1996) 2933–2936.

[23] R.F. Clayton, A. Owsianska, J. Aitken, S. Graham, D. Bhella, A.H. Patel, Analysis of antigenicity and topology of E2 glycoprotein present on recombinant hepatitis C virus-like particles, J. Virol. 76 (2002) 7672–7682.

[24] P. Pileri, Y. Uematsu, S. Campagnoli, G. Galli, F. Falugi, R. Petracca, A.-J. Weiner, M. Houghton, D. Rosa, G. Grandi, S. Abrignani, Binding of hepatitis C virus to CD81, Science 282 (1998) 938–941.

[25] D. Lavillette, Y. Morice, G. Germanidis, P. Donot, A. Soulier, E. Pagkalos, G. Sakellariou, L. Intrator, B. Bartosch, J.-M. Pawlotsky, F.-L. Cosset, Human serum facilitates hepatitis C virus infection, and neutralizing responses inversely correlate with viral replication kinetics at the acute phase of hepatitis C virus infection, J. Virol. 79 (2005) 6023–6034.

[26] Z. Stamataki, C. Shannon-Lowe, J. Shaw, D. Mutimer, A.-B. Rickinson, J. Gordon, D.-H. Adams, P. Balfe, J.-A. McKeating, Hepatitis C virus association with peripheral blood B lymphocytes potentiates viral infection of liver-derived hepatoma cells, Blood 113 (2009) 585–593.

[27] E. Scarselli, H. Ansuini, R. Cerino, R.-M. Roccasecca, S. Acali, G. Filocamo, C. Traboni, A. Nicosia, R. Cortese, A. Vitelli, The human scavenger receptor class B type I is a novel candidate receptor for the hepatitis C virus, EMBO. J. 21 (2002) 5017–5025.

[28] M.-J. Evans, T. von Hahn, D.-M. Tscherne, A.-J. Syder, M. Panis, B. Wolk, T. Hatziioannou, J.-A. McKeating, P.-D. Bieniasz, C.-M. Rice, Claudin-1 is a hepatitis C virus co-receptor required for a late step in entry, Nature 446 (2007) 801–805.

[29] J.-T. Blackard, N. Kemmer, K.-E. Sherman, Extrahepatic replication of HCV: insights into clinical manifestations and biological consequences, Hepatology 44 (2006) 15–22.

[30] T. Kato, T. Date, M. Miyamoto, A. Furusaka, K. Tokushige, M. Mizokami, T. Wakita, Efficient replication of the genotype 2a hepatitis C virus subgenomic replicon, Gastroenterology 125 (2003) 1808–1817.

[31] H. Aizaki, S. Nagamori, M. Matsuda, H. Kawakami, O. Hashimoto, H. Ishiko, M. Kawada, T. Matsuura, S. Hasumura, Y. Matsuura, T. Suzuki, T. Miyamura, Production and release of infectious hepatitis C virus from human liver cell cultures in the three-dimensional radial-flow bioreactor, Virology 314 (2003) 16–25.

nature immunology

The IκB kinase complex regulates the stability of cytokine-encoding mRNA induced by TLR–IL-1R by controlling degradation of regnase-1

Hidenori Iwasaki[1,2], Osamu Takeuchi[1,3], Shunsuke Teraguchi[1,4], Kazufumi Matsushita[1,6], Takuya Uehata[1,5], Kanako Kuniyoshi[1,3], Takashi Satoh[1], Tatsuya Saitoh[1,3], Mutsuyoshi Matsushita[2], Daron M Standley[4] & Shizuo Akira[1,3]

Toll-like receptor (TLR) signaling activates the inhibitor of transcription factor NF-κB (IκB) kinase (IKK) complex, which governs NF-κB-mediated transcription during inflammation. The RNase regnase-1 serves a critical role in preventing autoimmunity by controlling the stability of mRNAs that encode cytokines. Here we show that the IKK complex controlled the stability of mRNA for interleukin 6 (IL-6) by phosphorylating regnase-1 in response to stimulation via the IL-1 receptor (IL-1R) or TLR. Phosphorylated regnase-1 underwent ubiquitination and degradation. Regnase-1 was reexpressed in IL-1R- or TLR-activated cells after a period of lower expression. Regnase-1 mRNA was negatively regulated by regnase-1 itself via a stem-loop region present in the regnase-1 3′ untranslated region. Our data demonstrate that the IKK complex phosphorylates not only IκBα, thereby activating transcription, but also regnase-1, thereby releasing a 'brake' on IL-6 mRNA expression.

Inflammatory responses are rapidly elicited in response to infection by various pathogens and cellular stimuli[1–3]. Inflammation is mediated by proinflammatory cytokines such as tumor necrosis factor (TNF), interleukin 1β (IL-1β) and IL-6. Expression of cytokines is suppressed in resting cells of the innate immune system, whereas it is rapidly induced in response to infection by pathogens via a set of pattern-recognition receptors, such as Toll-like receptors (TLRs), helicase RIG-I–like receptors and biosensor Nod–like receptors.

The cytoplasmic portion of TLRs, the Toll–IL-1R domain, is homologous to that of the IL-1 receptor (IL-1R)[4]. IL-1R and all TLRs except TLR3 trigger intracellular signaling pathways by recruiting the adaptor MyD88. IL-1R-associated kinase 4 (IRAK4) then associates with MyD88 and activates IRAK1 and IRAK2 (ref. 5). The IRAKs then dissociate from MyD88 and interact with TRAF6, which acts as an E3 ubiquitin protein ligase[6]. Together with an E2 ubiquitin-conjugating enzyme complex composed of Ubc13 and Uev1A, TRAF6 catalyzes the formation of a lysine 63 (K63)-linked polyubiquitin chain on TRAF6 itself as well as the generation of an unconjugated free polyubiquitin chain[7]. A complex of the kinase TAK1 and the TAK1-binding proteins TAB1, TAB2 and TAB3 is activated by the unconjugated free K63 polyubiquitin chain and phosphorylates inhibitor of transcription factor NF-κB (IκB) kinase-β (IKKβ) and mitogen-activated protein kinase (MAP) kinase kinase 6 (ref. 6). In addition, linear ubiquitination of the NF-κB modulator IKKγ (NEMO) by a linear ubiquitin-chain assembly complex composed of HOIP, HOIL-1L and SHARPIN is required for activation of NF-κB[8–10]. Subsequently, the IKK complex, composed of IKKα, IKKβ and NEMO, phosphorylates the NF-κB-inhibitory protein IκBα on a DSGXXS motif (where 'X' is any amino acid)[11,12]. Phosphorylated IκBα undergoes ubiquitination by the the E3 ligase β-TrCP complex (β-transducin repeat–containing protein; also known as FBW1) and is degraded by the proteasome system, which thereby frees NF-κB to translocate to the nucleus and activate the transcription of genes encoding proinflammatory cytokines[11–15]. Activation of the MAP kinase cascade is responsible for the formation of another transcription factor complex, AP-1, that targets genes encoding cytokines. Signaling via the TNF receptor (TNFR) also leads to the activation of NF-κB by ubiquitination of the kinase RIP1, followed by activation of the TAK1 complex and linear ubiquitination of NEMO[8,16,17].

In addition to being controlled by transcriptional activation, cytokine-encoding mRNAs are controlled at the level of mRNA itself[18]. Proinflammatory cytokine–encoding mRNAs tend to have short half-lives, and mRNA stability is important for controlling the strength and duration of inflammation[19]. For example, tristetraprolin associates with AU-rich elements present in the 3′ untranslated regions (UTRs) of TNF mRNA and destabilizes TNF mRNA[20,21]. The cytoplasmic protein encoded by *Zc3h12a* is composed of a PIN-like

[1]Laboratory of Host Defense, World Premier International Immunology Frontier Research Center, Osaka University, Osaka, Japan. [2]Central Pharmaceutical Research Institute, Japan Tobacco, Osaka, Japan. [3]Research Institute for Microbial Diseases, Osaka University, Osaka, Japan. [4]Laboratory of Systems Immunology, World Premier International Immunology Frontier Research Center, Osaka University, Osaka, Japan. [5]Department of Geriatric Medicine and Nephrology, Osaka University Graduate School of Medicine, Osaka, Japan. [6]Present address: Laboratory of Allergic Diseases, Institute for Advanced Medical Sciences, Hyogo College of Medicine, Hyogo, Japan. Correspondence should be addressed to O.T. (otake@biken.osaka-u.ac.jp) or S.A. (sakira@biken.osaka-u.ac.jp).

Received 20 May; accepted 15 September; published online 30 October 2011; doi:10.1038/ni.2137

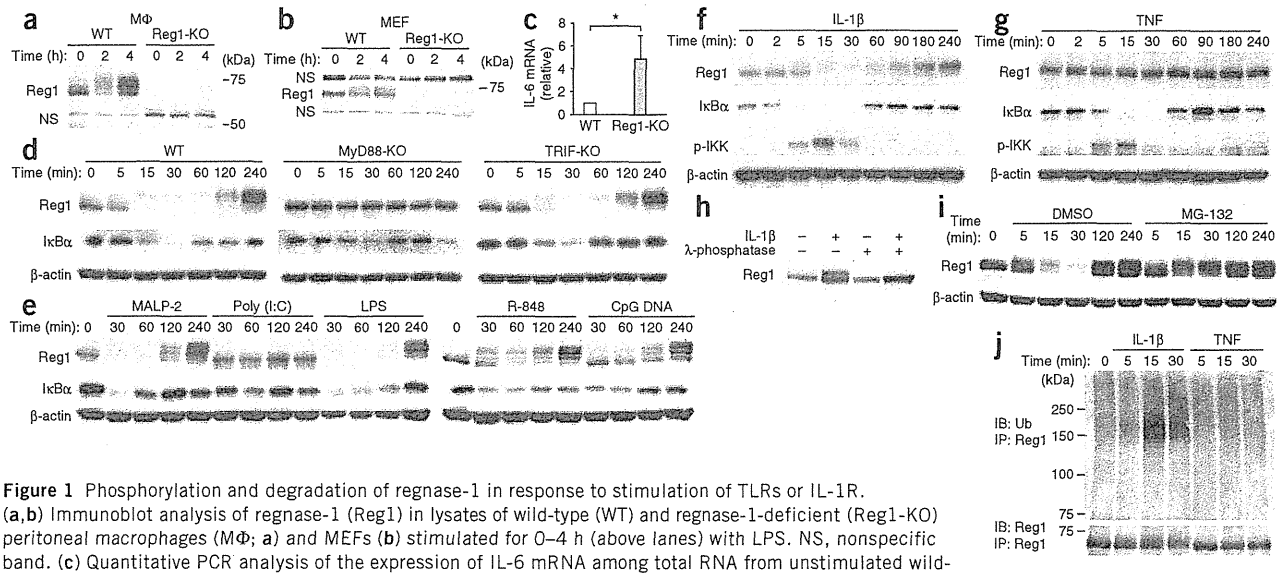

Figure 1 Phosphorylation and degradation of regnase-1 in response to stimulation of TLRs or IL-1R. (**a**,**b**) Immunoblot analysis of regnase-1 (Reg1) in lysates of wild-type (WT) and regnase-1-deficient (Reg1-KO) peritoneal macrophages (MΦ; **a**) and MEFs (**b**) stimulated for 0–4 h (above lanes) with LPS. NS, nonspecific band. (**c**) Quantitative PCR analysis of the expression of IL-6 mRNA among total RNA from unstimulated wild-type and regnase-1-deficient macrophages .*$P < 0.05$ (Student's *t*-test). (**d**) Immunoblot analysis of regnase-1, IκBα and β-actin (loading control) in wild-type, MyD88-deficient (MyD88-KO) and TRIF-deficient (TRIF-KO) macrophages stimulated for 0–240 min (above lanes) with LPS. (**e**) Immunoblot analysis of regnase-1, IκBα and β-actin in lysates of wild-type peritoneal macrophages stimulated for 0–240 min (above lanes) with MALP-2 (10 ng/ml), poly(I:C) (100 μg/ml), LPS (100 ng/ml), R-848 (10 nM) or CpG DNA (1 μM). (**f**,**g**) Immunoblot analysis of regnase-1, IκBα, phosphorylated (p-) IKK and β-actin in HeLa cells stimulated for 0–240 min (above lanes) with IL-1β (10 ng/ml; **f**) or TNF (10 ng/ml; **g**). (**h**) Immunoblot analysis of regnase-1 in HeLa cell lysates left unstimulated (–) or stimulated (+) with IL-1β and left untreated (–) or treated (+) with λ-phosphatase. (**i**) Immunoblot analysis of regnase-1 in HeLa cells pretreated with 0.1% dimethyl sulfoxide (DMSO) or the proteasome inhibitor MG-132 (1 μM), then stimulated for 0–240 min (above lanes) with IL-1β. (**j**) Immunoassay of lysates of HeLa cells stimulated for 0–30 min (above lanes) with IL-1β or TNF, followed by immunoprecipitation (IP) with anti-regnase-1 and immunoblot analysis (IB) with antibody to ubiquitin (Ub) or Reg1. Data are representative of three to five independent experiments (error bars (**c**), s.d.).

RNase domain and a CCCH-type zinc-finger domain[22]. As its RNase activity is directly responsible for regulating cytokine mRNA abundance, we have called this protein regulatory RNase 1 (regnase-1). The production of IL-6 and the p40 subunit of IL-12 in response to TLR ligands is much greater in regnase-1-deficient (*Zc3h12a*$^{-/-}$) macrophages[22]. The decay of IL-6 mRNA is impaired in regnase-1-deficient macrophages, and regnase-1 destabilizes mRNA via a conserved element independently of AU-rich elements present in the 3′ UTR of IL-6. Regnase-1-deficient mice spontaneously develop severe autoimmune inflammatory disease, which indicates that regnase-1-mediated control of mRNA expression has an essential role in maintaining homeostasis.

Although expression of regnase-1 mRNA is induced in response to stimulation with TLR ligands, the regulation of regnase-1 protein during the course of inflammation has not been clarified. In this study, we found that regnase-1 was rapidly degraded in response to stimulation with IL-1β or TLR ligands but not in response to TNF. Degradation of regnase-1 protein was important for higher expression of IL-6 mRNA. We identified IKKα,β as the kinase that induced ubiquitin-proteasome-mediated degradation of regnase-1 via β-TrCP. Regnase-1 mRNA was reexpressed about 240 min after stimulation of the TLR or IL-1R. Regnase-1 mRNA was targeted for degradation by regnase-1 protein. We generated a mathematical model in which the IKK complex phosphorylates not only IκBα, thereby activating transcription of genes encoding cytokines, but also regnase-1, thereby releasing the 'brake' on IL-6 mRNA expression. Moreover, as expression of the gene encoding regnase-1 was regulated by NF-κB, regnase-1 effectively functions as a 'molecular timer' that allows rapid generation of IL-6 mRNA during acute inflammation but inhibits sustained IL-6 production.

RESULTS

Modification of regnase-1 in response to TLR or IL-1R stimulation

To examine the expression of regnase-1 protein, we did immunoblot analysis of thioglycollate-elicited peritoneal macrophages and mouse embryonic fibroblasts (MEFs) from wild-type and regnase-1-deficient (*Zc3h12a*$^{-/-}$) mice. We confirmed the lack of regnase-1 expression in regnase-1-deficient peritoneal macrophages and MEFs (**Fig. 1a,b**). Notably, regnase-1 protein was expressed even in unstimulated macrophages and MEFs. In addition, regnase-1 protein was expressed in mouse thymus, spleen, lymph nodes and lungs (**Supplementary Fig. 1**). IL-6 mRNA was fivefold more abundant in regnase-1-deficient macrophages than wild-type macrophages even without stimulation (**Fig. 1c**), which suggested that expression of regnase-1 protein in unstimulated cells was required for the suppression of subtle inflammatory reactions. That hypothesis is consistent with the observed spontaneous development of autoimmune disease in regnase-1-deficient mice. When we looked closely at changes in regnase-1 expression, we found that the mobility of regnase-1 protein changed rapidly in response to lipopolysaccharide (LPS) and disappeared within 15 min of stimulation (**Fig. 1d**). Subsequently, regnase-1 reappeared within 120 min of stimulation, although most regnase-1 protein migrated slowly in the gel, which indicated that regnase-1 underwent some form of modification. It is well known that stimulation via TLR or IL-1β induces rapid degradation of IκBα protein and is followed by re-expression, which allows the nuclear translocation of NF-κB[14,15]. The kinetics of the LPS-induced regnase-1 expression was similar to that of IκBα in wild-type macrophages and MEFs (**Fig. 1d** and **Supplementary Fig. 2**). LPS is recognized by TLR4 and triggers distinct signaling pathways via the adaptors MyD88 and TRIF[4]. Both MyD88-dependent and TRIF-dependent pathways are

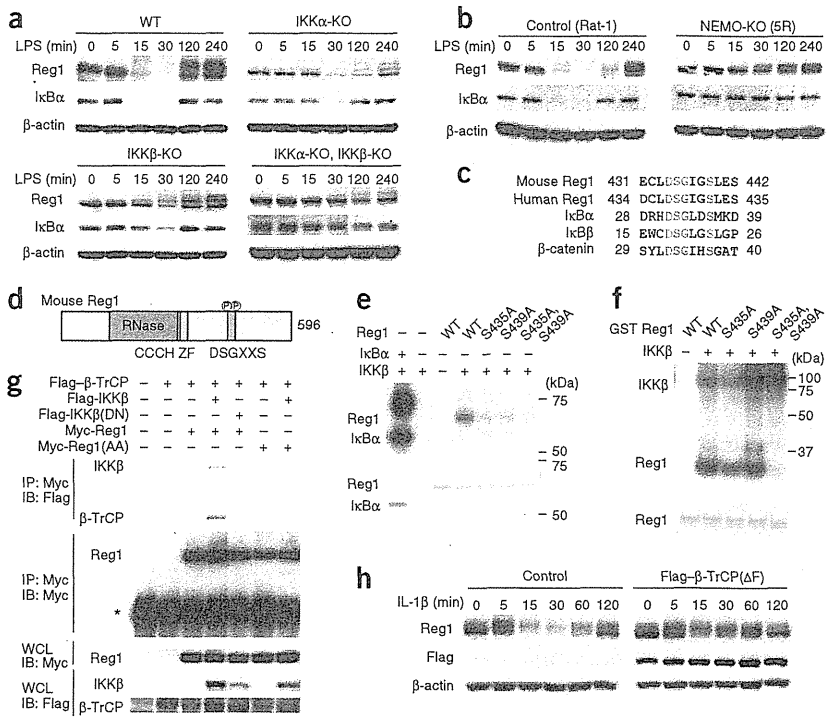

Figure 2 The IKK complex is essential for regnase-1 phosphorylation. (**a**,**b**) Immunoblot analysis of regnase-1, IκBα and β-actin in MEFs from wild-type mice or mice deficient in IKKα (IKKα-KO), IKKβ (IKKβ-KO) or both IKKα and IKKβ (IKKα-KO,IKKβ-KO; **a**) and of Rat-1 (NEMO-sufficient) cells and 5R (NEMO-deficient) cells (**b**), stimulated for 0–240 min (above lanes) with LPS. (**c**) Alignment of DSGXXS motifs (red) in mouse and human regnase-1 and mouse IκBα, IκBβ and β-catenin. (**d**) Regnase-1 domains, including the RNase domain (green), the zinc-finger domain (CCCH ZF; orange) and the DSGXXS domain (red; 596 (far right) indicates total amino acids present). (**e**,**f**) *In vitro* kinase assay (top) of recombinant IKKβ and wild-type or mutant regnase-1 (**e**) or GST fusion proteins of wild-type or mutant regnase-1 (**f**), and SDS-PAGE and Coomassie blue staining (bottom) of wild-type and mutant regnase-1 (all corresponding to regnase-1 amino acids 430–441). kDa, kilodaltons. (**g**) Immunoassay of the association of regnase-1 and β-TrCP in HEK293 cells transfected with various combinations (above lanes) of expression plasmids for Flag-tagged β-TrCP (Flag–β-TrCP), wild-type IKKβ (Flag-IKKβ) or kinase-inactive IKKβ (Flag-IKKβ(DN)), and Myc-tagged wild-type regnase-1 (Myc-Reg1) or S435A,S439A mutant regnase-1 (Myc-Reg1(AA)), followed by immunoprecipitation of proteins from lysates with anti-Myc and immunoblot analysis with anti-Flag or anti-Myc. *, immunoglobulin heavy chain. Below, immunoblot analysis of whole-cell lysates (WCL) with anti-Myc or anti-Flag. (**h**) Immunoblot analysis of regnase-1, dominant negative β-TrCP(ΔF) and β-actin in HeLa cells expressing Flag-tagged β-TrCP(ΔF) or control plasmid and stimulated for 0–120 min (above lanes) with IL-1β. Data are representative of three to four independent experiments.

required for optimal LPS-mediated proinflammatory cytokine production, although each pathway results in the degradation of IκBα and activation of NF-κB[23]. Whereas we observed LPS-induced disappearance of IκBα in MyD88-deficient and TRIF-deficient macrophages, we observed the disappearance of regnase-1 in macrophages from TRIF-deficient mice but not those from MyD88-deficient mice (**Fig. 1d**). Downstream of MyD88, the kinases IRAK1 and IRAK2 or IRAK4 were required for the degradation of regnase-1 in response to LPS (**Supplementary Fig. 3**). In macrophages stimulated with ligands for various TLRs, including MALP-2 (TLR6-TLR2), poly (I:C) (TLR3), LPS (TLR4), R-848 (TLR7) or CpG DNA (TLR9), the modification and disappearance of regnase-1 were induced in response to all TLR ligands except poly (I:C) (**Fig. 1e**). Given that all TLRs except TLR3 signal via MyD88 (ref. 4), these results indicated that the MyD88-dependent signaling pathway was essential for the disappearance in regnase-1 expression. In contrast, stimulation of cells with chemokines and cytokines such as MCP-1, IL-6 and IFN-γ failed to induce changes in regnase-1 expression (**Supplementary Fig. 4**). Consistent with those observations, HeLa human cervical cancer cells stimulated with IL-1β showed modification and disappearance of regnase-1, but those stimulated with TNF did not (**Fig. 1f,g**). In contrast, degradation of IκBα was induced equivalently by IL-1β and TNF. We then investigated the mechanism by which regnase-1 was modified in response to stimulation via TLRs or IL-1R. Treatment of IL-1β-stimulated cell lysates with λ-phosphatase resulted in the disappearance of slowly migrating regnase-1 (**Fig. 1h**), which indicated that regnase-1 was phosphorylated in response to IL-1β. Treatment of HeLa cells with the proteasome inhibitor MG-132 resulted in considerable impairment in the decrease in regnase-1 (**Fig. 1i**), and immunoblot analysis showed that IL-1β induced the ubiquitination of regnase-1 but TNF did not (**Fig. 1j**). Thus, regnase-1 was rapidly phosphorylated in response to IL-1β and was degraded via the ubiquitin-proteasome pathway.

IKKβ can phosphorylate regnase-1 on a DSGXXS motif

We next searched for the kinase responsible for the phosphorylation and degradation of regnase-1. Neither modification nor degradation of regnase-1 was affected by pretreatment of HeLa cells with cycloheximide or actinomycin D (**Supplementary Fig. 5**), which indicated that modification of regnase-1 did not require IL-1β-mediated protein synthesis or gene transcription. Although MAP kinases such as Erk, Jnk and p38, as well as phosphoinositide-3-OH kinases, are activated in response to stimulation via TLRs or IL-1R, pretreatment of HeLa cells with inhibitors of those receptors failed to prevent the IL-1β-induced degradation and reappearance of regnase-1 (**Supplementary Fig. 6**). In contrast, treatment with the IKKβ inhibitor TPCA-1 inhibited the degradation of regnase-1 (**Supplementary Fig. 6**). Therefore, we investigated the contribution of the IKK complex to regnase-1 degradation. MEFs lacking IKKα showed unimpaired regnase-1 degradation in response to LPS, whereas IKKβ-deficient MEFs showed partially impaired degradation of regnase-1 and IκBα (**Fig. 2a**). However, cells lacking both IKKα and IKKβ did not show any degradation of regnase-1 or IκBα in response to LPS (**Fig. 2a**). Nevertheless, slowly migrating regnase-1 still appeared in the late phase of stimulation, which suggested that another kinase phosphorylated regnase-1 without affecting its degradation. Consistent with that, NEMO-deficient Rat-1 rat fibroblasts (5R cells)[24] did not have less regnase-1 or IκBα after LPS stimulation than did control NEMO-sufficient Rat-1 cells (**Fig. 2b**), which indicated that the IKK complex was essential for the degradation of regnase-1. Sequence analysis showed that regnase-1

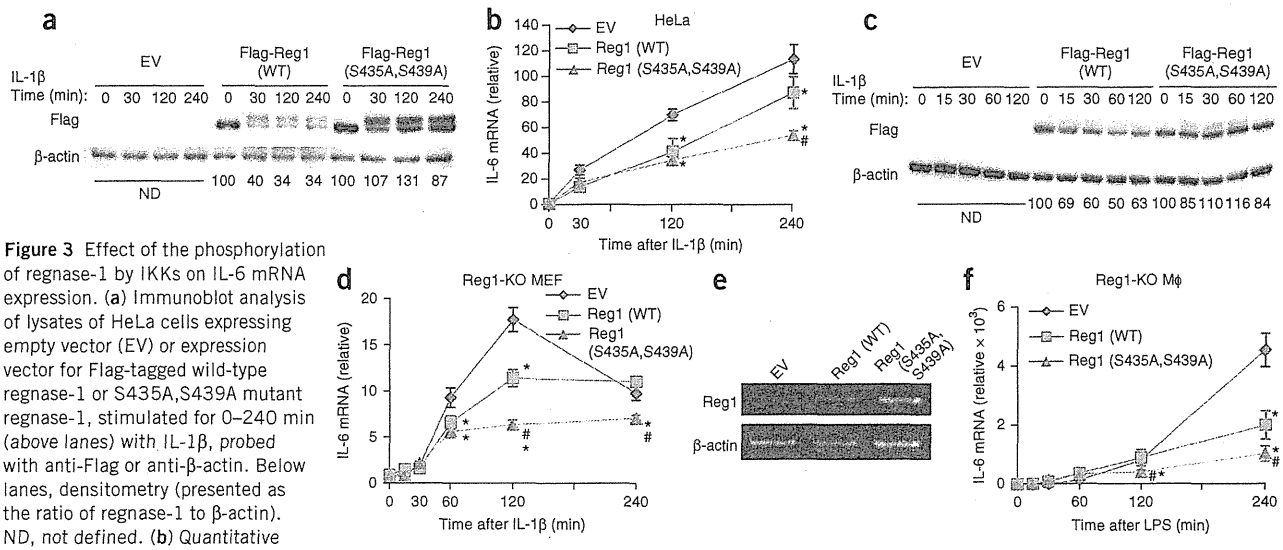

Figure 3 Effect of the phosphorylation of regnase-1 by IKKs on IL-6 mRNA expression. (**a**) Immunoblot analysis of lysates of HeLa cells expressing empty vector (EV) or expression vector for Flag-tagged wild-type regnase-1 or S435A,S439A mutant regnase-1, stimulated for 0–240 min (above lanes) with IL-1β, probed with anti-Flag or anti-β-actin. Below lanes, densitometry (presented as the ratio of regnase-1 to β-actin). ND, not defined. (**b**) Quantitative PCR analysis of the expression of IL-6 mRNA among total RNA from the cells in **a**, presented relative to 18S RNA. (**c**) Immunoblot analysis of lysates of regnase-1-deficient MEFs infected with control retrovirus (EV) or retrovirus expressing Flag-tagged wild-type regnase-1 or the S435A,S439A regnase-1 mutant, then stimulated for 0–120 min (above lanes) with IL-1β, probed with anti-Flag or β-actin. Below lanes, densitometry (as in **a**). (**d**) Quantitative PCR analysis as in **b** of total RNA from the cells in **c**. (**e**) Semiquantitative RT-PCR analysis of wild-type regnase-1 and S435A,S439A mutant regnase-1 in macrophages prepared from regnase-1-deficient bone marrow cells infected with retrovirus as in **c**. (**f**) Quantitative PCR analysis (as in **b**) of the cells in **e**, stimulated for 0–240 min (horizontal axis) with LPS. $*P < 0.05$, empty vector versus regnase-1 (wild type or S435A,S439A), and $P < 0.05$, wild-type regnase-1 versus S435A,S439A regnase-1 (Student's *t*-test). Data are representative of three to four independent experiments with similar results (mean ± s.d. of triplicates in **b**,**d**,**f**).

had the canonical DSGXXS motif known to be phosphorylated by IKKs[11] (**Fig. 2c**). This motif in regnase-1 was located in an unstructured region, C-terminal to the nuclease and CCCH-type zinc-finger domains (**Fig. 2d**), and the motif was conserved among species from zebrafish to humans (**Supplementary Fig. 7**). As expected, IKKβ and IKKα phosphorylated synthesized full-length regnase-1 protein and a glutathione *S*-transferase (GST) fusion peptide corresponding to amino acids 430–441, including the DSGXXS motif, *in vitro* (**Fig. 2e,f** and data not shown). Furthermore, the phosphorylation of mouse regnase-1 was attenuated by the substitution of serine residues Ser435 and Ser439 with alanine (S435A,S439A; **Fig. 2e,f**), which indicated that the two serine residues present in the DSGXXS motif were the targets of the phosphorylation of regnase-1 by IKKs. In addition, coimmunoprecipitation analysis showed that IKKβ interacted with regnase-1 endogenously (**Supplementary Fig. 8a,b**). Stimulation with IL-1β failed to change this interaction, which suggested that regnase-1 formed a stable complex with IKKβ in resting cells. Although the DSGXXS motif is also known to be phosphorylated by another kinase, GSK3β[13], treatment with the GSK3β inhibitor LiCl failed to inhibit IL-1β-mediated degradation of regnase-1 (**Supplementary Fig. 9**). It is well known that the phosphorylated DSGXXS sequence is subsequently recognized by the E3 ligase β-TrCP for polyubiquitination[13]. To determine if regnase-1 interacts with β-TrCP, we expressed β-TrCP and regnase-1 in HEK293 human embryonic kidney cells and found that β-TrCP precipitated together with regnase-1 only when wild-type IKKβ was coexpressed (**Fig. 2g**). In contrast, coexpression of kinase-inactive IKKβ did not induce an association between β-TrCP and regnase-1. Furthermore, mutant regnase-1 (S435A,S439A)

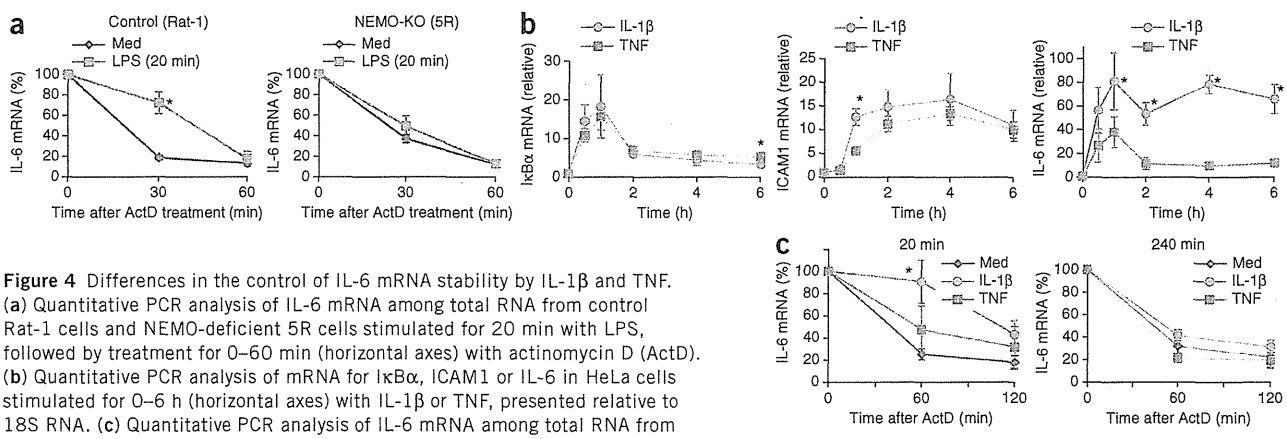

Figure 4 Differences in the control of IL-6 mRNA stability by IL-1β and TNF. (**a**) Quantitative PCR analysis of IL-6 mRNA among total RNA from control Rat-1 cells and NEMO-deficient 5R cells stimulated for 20 min with LPS, followed by treatment for 0–60 min (horizontal axes) with actinomycin D (ActD). (**b**) Quantitative PCR analysis of mRNA for IκBα, ICAM1 or IL-6 in HeLa cells stimulated for 0–6 h (horizontal axes) with IL-1β or TNF, presented relative to 18S RNA. (**c**) Quantitative PCR analysis of IL-6 mRNA among total RNA from HeLa cells stimulated for 20 or 240 min (above plots) with medium alone (Med), IL-1β or TNF, then treated for 0–120 min (horizontal axes) with actinomycin D. $*P < 0.05$ (Student's *t*-test). Data are from three independent experiments (mean ± s.d.).

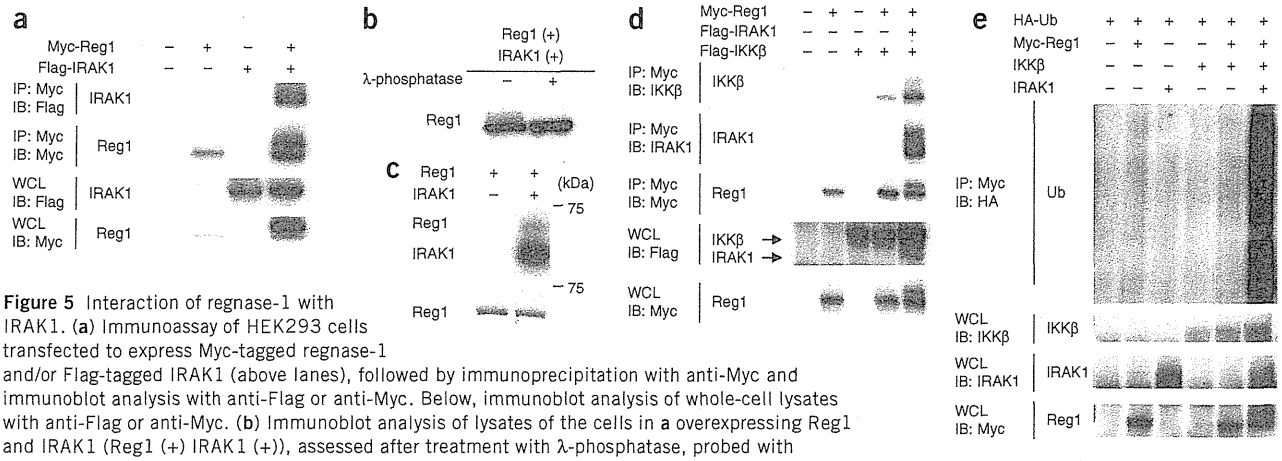

Figure 5 Interaction of regnase-1 with IRAK1. (**a**) Immunoassay of HEK293 cells transfected to express Myc-tagged regnase-1 and/or Flag-tagged IRAK1 (above lanes), followed by immunoprecipitation with anti-Myc and immunoblot analysis with anti-Flag or anti-Myc. Below, immunoblot analysis of whole-cell lysates with anti-Flag or anti-Myc. (**b**) Immunoblot analysis of lysates of the cells in **a** overexpressing Reg1 and IRAK1 (Reg1 (+) IRAK1 (+)), assessed after treatment with λ-phosphatase, probed with anti-Myc. (**c**) *In vitro* kinase assay of recombinant regnase-1 and IRAK1 (top), and SDS-PAGE and Coomassie blue staining of regnase-1 (bottom). (**d**) Immunoassay of HEK293 cells transfected to express Myc-tagged regnase-1 and/or Flag-tagged IRAK1 or IKKβ (above lanes), followed by immunoprecipitation from lysates with anti-Myc and immunoblot analysis with anti-IKKβ, anti-IRAK1 or anti-Myc. Below, immunoblot analysis of whole-cell lysates with anti-Flag or anti-Myc. (**e**) Immunoassay of HEK293 cells transfected to express hemagglutinin-tagged ubiquitin (HA-Ub), Myc-tagged regnase-1 and/or IKKβ or IRAK1 (above lanes), followed by immunoprecipitation from lysates with anti-Myc and immunoblot analysis of ubiquitin (with anti-HA). Below, immunoblot analysis of whole-cell lysates with anti-IKKβ, anti-IRAK1 or anti-Myc. Data are representative of three to four independent experiments.

failed to interact with β-TrCP and IKKβ (**Fig. 2g**), which suggested that phosphorylation of the DSGXXS sequence present in regnase-1 was essential for its interaction with β-TrCP. To evaluate the role of β-TrCP in the degradation of regnase-1, we used a β-TrCP mutant that fails to associate with other subunits of the E3 ubiquitin ligase complex and functions as a dominant-negative form (β-TrCP(ΔF))[25]. Overexpression of β-TrCP(ΔF) in HeLa cells resulted in less IL-1β-mediated degradation of regnase-1 without affecting the phosphorylation (**Fig. 2h**). Collectively, these results indicated that IKKα,β phosphorylated regnase-1 on its canonical DSGXXS sequence and that β-TrCP was responsible for activation of the ubiquitin-proteasome pathway.

Regnase-1 degradation controls IL-6 mRNA expression

IL-6 mRNA is stabilized in regnase-1-deficient macrophages[22]. To examine the role of IKK-mediated phosphorylation and degradation of regnase-1 in controlling the stability of IL-6 mRNA, we expressed wild-type regnase-1 and the S435A,S439A regnase-1 mutant in HeLa cells. Whereas wild-type regnase-1 was degraded in response to IL-1β stimulation, the S435A,S439A mutant was resistant to the stimuli (**Fig. 3a**). Notably, the S435A,S439A mutant protein still migrated slowly after stimulation, which indicated amino acids other than Ser435 and Ser439 were phosphorylated by an unknown kinase without affecting regnase-1 degradation. Although the expression of IL-6 mRNA decreased even when wild-type regnase-1 was expressed, expression of the S435A,S439A mutant suppressed IL-6 mRNA expression more in response to IL-1β (**Fig. 3b**). Next we expressed wild-type regnase-1 and the S435A,S439A mutant via retrovirus in regnase-1-deficient MEFs. Whereas wild-type regnase-1 was degraded in response to IL-1β, the S435A,S439A mutant was resistant to degradation (**Fig. 3c**). Consistent with the results obtained with HeLa cells, the S435A,S439A mutant was more potent in suppressing IL-6 mRNA expression than was wild-type regnase-1 (**Fig. 3d**). Furthermore, wild-type regnase-1 and the S435A,S439A mutant expressed via retrovirus in regnase-1-deficient macrophages acted similarly. Whereas expression of wild-type regnase-1 also partially inhibited IL-6 expression in response to LPS, the S435A,S439A mutant was more potent in suppressing IL-6 mRNA expression (**Fig. 3e,f**). These results indicated that IKK-mediated phosphorylation of regnase-1 was involved in augmenting IL-6 mRNA expression in the course of TLR- or IL-1R-mediated inflammation.

The IKK complex enhances IL-6 mRNA stability

Next we determined if the IKK complex controlled the stability of IL-6 mRNA in addition to controlling transcription. IL-6 mRNA was more stable in wild-type (Rat-1) cells stimulated for 20 min with LPS than in unstimulated cells, and the mRNA half-life was longer (**Fig. 4a**). In contrast, cells lacking NEMO (5R cells) failed to stabilize IL-6 mRNA in response to stimulation for 20 min with LPS (**Fig. 4a**), which indicated that the IKK complex also regulated the stability of cytokine mRNA in addition to controlling transcription. As IL-1β induced degradation of regnase-1 within 15 min, but not TNF did not, we compared the expression of a set of NF-κB-inducible genes in HeLa cells in response to stimulation with IL-1β or TNF. Phosphorylation of IKKs was induced with similar kinetics in response to IL-1β or TNF (**Fig. 1f,g**). Although IL-1β and TNF induced IκBα mRNA and the integrin ligand ICAM1 with similar kinetics, consistent with a published report[19], the expression of IL-6 mRNA was higher in response to IL-1β stimulation (**Fig. 4b**). When we measured the stability of IL-6 mRNA 20 min after stimulation with IL-1β or TNF, we found that IL-1β extended the half-life of IL-6 mRNA much more than TNF did (**Fig. 4c** and **Table 1**). Consistent with the reappearance of regnase-1 protein 60–90 min after stimulation with IL-1β (**Fig. 1f**), the half-life of IL-6 mRNA at 240 min was similar after stimulation with IL-1β or TNF (**Fig. 4c** and **Table 1**), which indicated that the

Table 1 Change in IL-6 mRNA half-life in response to IL-1β stimulation in HeLa cells

Stimulation	20 min	240 min
Medium alone	40.6 ± 3.3	44.6 ± 5.4
IL-1β	110.9 ± 11.6	51.7 ± 4.2
TNF	48.0 ± 4.4	37.4 ± 1.8

Half-life of IL-6 mRNA (in min) in HeLa cells before (Medium alone) or 20 or 240 min after stimulation with IL-1β or TNF (calculated based on the kinetic changes in **Fig. 4c**). Data are from three independent experiments (mean ± s.d.).

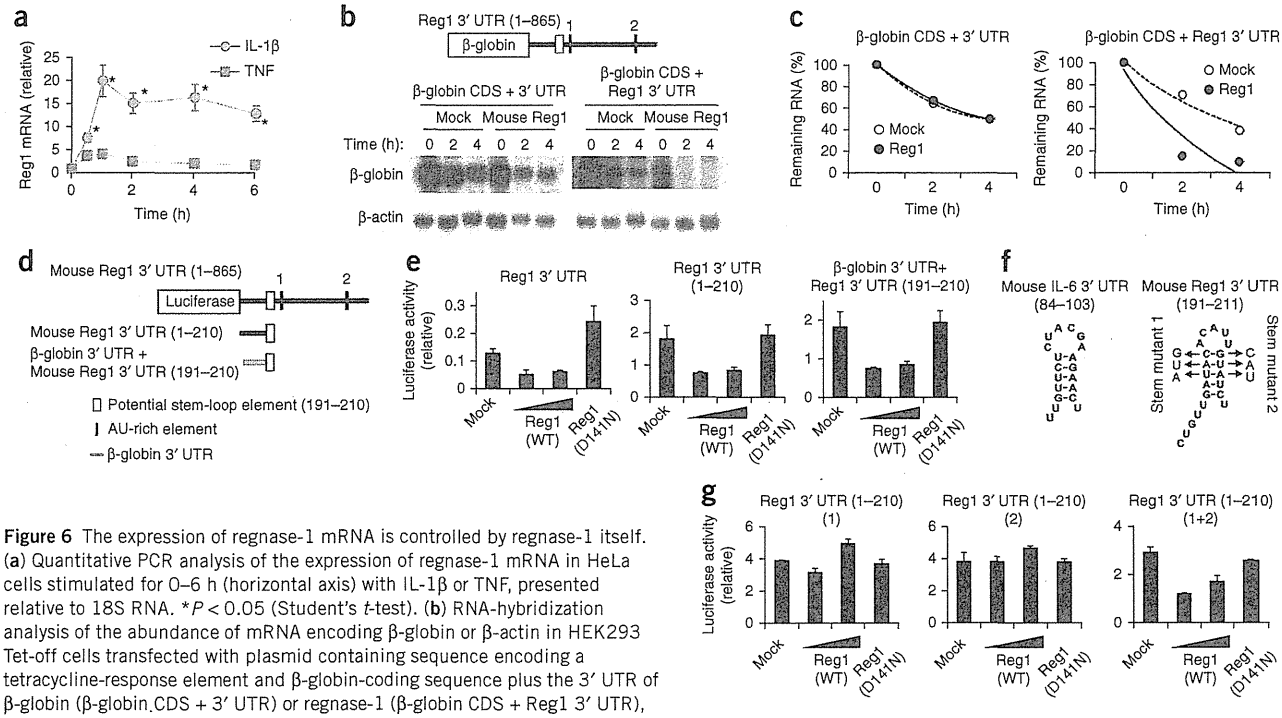

Figure 6 The expression of regnase-1 mRNA is controlled by regnase-1 itself. (**a**) Quantitative PCR analysis of the expression of regnase-1 mRNA in HeLa cells stimulated for 0–6 h (horizontal axis) with IL-1β or TNF, presented relative to 18S RNA. $*P < 0.05$ (Student's *t*-test). (**b**) RNA-hybridization analysis of the abundance of mRNA encoding β-globin or β-actin in HEK293 Tet-off cells transfected with plasmid containing sequence encoding a tetracycline-response element and β-globin-coding sequence plus the 3′ UTR of β-globin (β-globin CDS + 3′ UTR) or regnase-1 (β-globin CDS + Reg1 3′ UTR), together with control empty plasmid (Mock) or expression plasmid for regnase-1 (Mouse Reg1), then divided 3 h after transfection and incubated for an additional 20 h, followed by treatment (time, above lanes) with doxycycline (1 μg/ml). (**c**) Quantification of the autoradiographs in **b**, presented as the ratio of β-globin to β-actin. (**d**) The 3′ UTR of mouse regnase-1 mRNA (positions 1–865) and deletion constructs. (**e**) Luciferase activity of HEK293 cells transfected for 48 h with luciferase reporter plasmids as in **d** (top), together with control plasmid (Mock) or expression plasmid for wild-type regnase-1 or a nuclease-inactive mutant of regnase-1 (D141N); results are presented relative to renilla luciferase activity. (**f**) Predicted stem-loop structure of the regnase-1-responsive element in the 3′ UTR of IL-6 mRNA (left) or regnase-1 mRNA (right), pus mutations leading to disruption of the regnase-1 stem-loop structure (Stem mutant 1 and 2). (**g**) Luciferase activity of HEK293 cells transfected for 48 h with luciferase reporter plasmids containing sequence as in **f** (stem mutants alone (1 or 2) or together (1+2)), together with expression plasmids as in **e** (presented as in **e**). Data are representative of three independent experiments (**a**–**c**) or three independent experiments with similar results (**e**,**g**; error bars, s.d. of duplicates).

kinetics of IL-6 mRNA stability correlated well with the abundance of regnase-1 protein in response to stimulation with IL-1β or TNF. We further investigated the role of regnase-1 degradation in the stability of IL-6 mRNA by comparing the contributions of MyD88 and TRIF in response to LPS. The half-life of IL-6 mRNA was extended in response to LPS in control and TRIF-deficient MEFs (**Supplementary Table 1**). In contrast, LPS did not affect the half-life of IL-6 mRNA in MyD88-deficient cells, consistent with the status of regnase-1 protein expression. These results suggested that the lower abundance of regnase-1 protein in response to simulation with IL-1β or TLR contributed to the greater stability of IL-6 mRNA. Collectively, these results indicated that the IKK complex activated not only the transcription of genes encoding cytokines by the IκBα–NF-κB pathway but also stabilized IL-6 mRNA by degrading regnase-1 in response to stimulation via the IL-1R or TLR (**Supplementary Fig. 10**).

IRAK1 interacts with and phosphorylates regnase-1

We next investigated the mechanism by which regnase-1 was degraded by stimulation with IL-1R or TLR but not by TNFR. The data presented above indicated that activation of the IKK complex alone was not sufficient to induce regnase-1 modification. Whereas signaling molecules downstream of TAK1 are shared by IL-1R, TLR and TNFR, signaling molecules such as MyD88 and IRAKs are activated by IL-1R and TLR but not by TNFR. It has been reported that IRAKs control mRNA stability in addition to activating NF-κB[26,27]. However, cells that lack both IRAK1 and IRAK2 are still able to activate NF-κB downstream of MyD88 (ref. 5). As MyD88, IRAK1 and IRAK2 were all necessary for regnase-1 degradation, the IRAKs degraded regnase-1 by a mechanism independent of simple activation of the IKK complex. Thus, we hypothesized that modification of regnase-1 by IRAKs is necessary for subsequent phosphorylation by the IKKs. When we overexpressed IRAK1 and regnase-1 in HEK293 cells, we observed that IRAK1 precipitated together with regnase-1 (**Fig. 5a**), which indicated that regnase-1 interacted with IRAK1. Further, the mobility of regnase-1 during electrophoresis through the gel changed when IRAK1 was coexpressed (**Fig. 5a**). Treatment of cell lysates with λ-phosphatase resulted in disappearance of regnase-1 protein that migrated more slowly (**Fig. 5b**), which suggested that regnase-1 was phosphorylated by IRAK1. We confirmed that finding by an *in vitro* kinase assay in which we incubated recombinant IRAK1 with regnase-1 and determined if IRAK1 modulated the interaction between regnase-1 and IKKβ (**Fig. 5c**). Coexpression of IRAK1 augmented the interaction between the regnase-1 and IKKβ (**Fig. 5d**).

Table 2 Change in regnase-1 mRNA half-life in response to IL-1β stimulation

Stimulation	20 min	240 min
Medium alone	49.2 ± 4.0	48.3 ± 5.3
IL-1β	132.1 ± 20.7	59.5 ± 6.7
TNF	60.1 ± 18.5	49.2 ± 11.6

Half-life of regnase-1 mRNA in HeLa cells before and 20 or 240 min after stimulation with IL-1β or TNF. Data are from three independent experiments (mean ± s.d.).

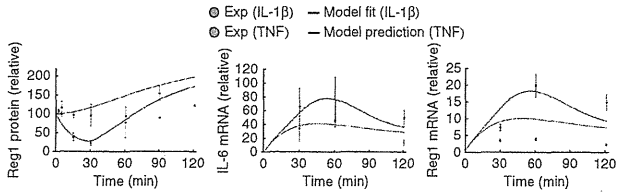

Figure 7 Computational modeling of the control of IL-6 mRNA expression by regnase-1. Expression of regnase-1 protein, IL-6 mRNA and regnase-1 mRNA in HeLa cells stimulated for 0–120 min (horizontal axes) with IL-1β (Exp (IL-1β)) or TNF (Exp (TNF)), followed by normalization to initial values (obtained from **Figs. 4b** and **6a**). Model fit (IL-1β), model values fit to the data after stimulation with IL-1β (fitted by COPASI 4.6 software for the simulation and analysis of biochemical networks and their dynamics[35]); Model prediction (TNF), corresponding model predictions for stimulation with TNF.

Furthermore, coexpression of IRAK1 resulted in considerable augmentation of the ubiquitination of regnase-1 induced by IKKβ (**Fig. 5e**). Collectively, these results suggested that IRAK1 facilitated regnase-1 ubiquitination mediated by IKKβ by direct interaction with and modification of regnase-1.

Regnase-1 protein controls regnase-1 mRNA

Once regnase-1 underwent rapid degradation in response to TLR or IL-1R stimuli, it reappeared within 60–120 min of stimulation. This required new synthesis of regnase-1 mRNA via transcription (**Supplementary Fig. 5**). Expression of regnase-1 mRNA in response to IL-1β is controlled by the transcription factors NF-κB and Elk-1 (ref. 28). Although NF-κB activation was induced similarly in HeLa cells in response to IL-1β or TNF (**Supplementary Fig. 11**), stimulation with IL-1β induced upregulation of regnase-1 mRNA, but stimulation with TNF did not (**Fig. 6a**). The half-life of regnase-1 mRNA was longer after 20 min of stimulation with IL-1β, but not after 20 min of stimulation with TNF (**Table 2**). In contrast, the half-life of regnase-1 mRNA was similar in unstimulated cells and those exposed to longer periods of stimulation with IL-1β (240 min; **Table 2**).

Those results prompted us to hypothesize that regnase-1 mRNA is a target of the regnase-1 RNase domain. To examine this possibility, we expressed constructs with β-globin-coding sequence and the 3′ UTR of regnase-1 or β-globin, plus the 'Tet-off' (tetracycline-regulated) gene-expression system (**Fig. 6b**). By halting new transcription with doxycycline, we were able to measure mRNA stability. Overexpression of regnase-1 resulted in rapid degradation of β-globin mRNA in the presence of the regnase-1 3′ UTR (**Fig. 6b,c**), which indicated that regnase-1 targeted regnase-1 mRNA via its 3′ UTR. Next we expressed luciferase reporter constructs with the entire 3′ UTR of regnase-1 (postions 1–865; numbered from the start of the 3′ UTR) in HEK293 cells (**Fig. 6d**). The luciferase activity decreased in response to coexpression of regnase-1 in a transfection dose-dependent manner (**Fig. 6e**). Furthermore, expression of a nuclease-inactive mutant of regnase-1 did not suppress the reporter activity (**Fig. 6e**), which indicated that regnase-1 controlled its own mRNA in a nuclease activity–dependent way. Next, by testing a set of luciferase constructs with truncation of the 3′ UTR of regnase-1, we found that positions 1–210 of the 3′ UTR produced regnase-1-mediated suppression, but positions 1–200 did not (**Supplementary Fig. 12**). We confirmed that the 3′ UTR (positions 192–210 of mouse regnase-1) was evolutionally conserved (**Supplementary Fig. 13**) and that the addition of this sequence to the β-globin 3′ UTR conferred responsiveness to regnase-1 overexpression (**Fig. 6e**). This sequence motif was predicted to form a stem-loop structure (**Fig. 6f**) like the regnase-1-responsive sequence in the 3′ UTR of IL-6 mRNA[22,29], and disruption of the stem-loop structure abrogated regnase-1-mediated suppression of the luciferase activity, whereas further insertion of mutations that restored the stem-loop structure 'rescued' the responsiveness of regnase-1 (**Fig. 6g**). These results suggested that the stem-loop structure present in the 3′ UTR of regnase-1 was required for regnase-1-mediated inhibition.

Mathematical modeling of the control of IL-6 mRNA

We next constructed a mathematical model that captured the activity of regnase-1 protein and regnase-1 and IL-6 mRNA based on biochemical equations with minimal assumptions (**Supplementary Fig. 14**). In the model, mRNA abundance was regulated via the digestion of mRNA by regnase-1 protein with experimentally determined degradation rates. The difference between stimulation with IL-1β and stimulation with TNF was described mathematically by constant degradation of regnase-1 protein for 30 min after stimulation with IL-1β, but not after stimulation with TNF. Whereas we determined the unknown parameters in the model by fitting only to the experimental data obtained after stimulation with IL-1β, the model qualitatively reproduced the kinetics after stimulation with TNF (**Fig. 7** and **Supplementary Table 2**). The differences in mRNA abundance after stimulation with IL-1β or TNF in this model resulted only from the digestion of mRNA by regnase-1 protein. These simulations indicated that our model captured the essence of the system dynamics.

DISCUSSION

Here we have shown that regnase-1 protein underwent dynamic modification in response to stimulation via TLRs or IL-1R. Regnase-1 was phosphorylated by the IKK complex, which led to its degradation by a ubiquitin-proteasome-dependent mechanism. Regnase-1 mutant proteins resistant to degradation showed more potency in suppressing IL-6 mRNA expression than did wild-type regnase-1. The expression of regnase-1 protein was induced in the later stage of TLR responses. Regnase-1 mRNA was controlled by regnase-1 protein via its 3′ UTR, which could contribute to reexpression of regnase-1 protein.

We found that expression of regnase-1 in resting cells prevented unwanted production of cytokines. The expression of IL-6 mRNA in unstimulated conditions was higher in regnase-1-deficient cells than in wild-type cells. This result suggested that transcriptional inhibition alone was not sufficient to shut down IL-6 mRNA completely. The trace amounts of proinflammatory cytokine–encoding mRNAs produced by background transcription should be degraded in resting cells by proteins such as regnase-1. Given that regnase-1-deficient mice spontaneously develop inflammatory disease, a dual locking system of inhibition of transcription and degradation of mRNA seems to be essential for the maintenance of homeostasis.

IKKs were identified as kinases responsible for the phosphorylation and degradation of IκBα, an inhibitor of NF-κB activation. The role of IKKs in the transcriptional activation of genes involved in inflammation has been studied extensively. In this study, we identified regnase-1 as a previously unsuspected substrate of IKK in response to activation via TLRs or IL-1R. It is notable that this single kinase complex regulated both gene transcription and mRNA stability in response to TLR stimulation. Although published studies have identified IKK substrates such as Bcl-10, SNAP23, p53 and IRF7 (refs. 30–33), only regnase-1 and IκBα were rapidly phosphorylated and degraded in response to activation of the IKK complex after stimulation via TLRs or IL-1β. A canonical DSGXXS motif is present in regnase-1 of various vertebrates, which suggests that the IKKβ-TrCP–mediated modification of regnase-1 is evolutionally conserved. Furthermore, rapid degradation

of regnase-1 allowed the cells to quickly express large amounts of cytokine mRNA in response to stimulation of TLRs or IL-1R.

We found that stimulation with IL-1β led to the degradation of regnase-1, but stimulation with TNF did not, although both cytokines activated the IKK complex. Furthermore, a MyD88-dependent signaling pathway was essential for extending the half-life of IL-6 mRNA, but a TRIF-dependent pathway was not, although both pathways led to IKK-mediated activation of NF-κB. We found that IRAK1 associated with and phosphorylated regnase-1. IRAK1 and IRAK2 were activated by IRAK4 and functioned redundantly in controlling the production of proinflammatory cytokines. It has been shown that IRAK1 as well as IRAK2 are critical for regulating the stability of cytokine-encoding mRNA, whereas TRAF6 is dispensable for IL-1α-induced stabilization of mRNA[26,27]. IRAK2 is reported to interact with the p38-activated kinase MK2, which inhibits the degradation of TNF mRNA by phosphorylating and sequestering tristetraprolin. Collectively, IRAKs may regulate mRNA stability by directly modulating various cellular proteins. However, further studies of the phosphorylation sites of regnase-1 are needed to identify the precise molecular mechanism by which IRAKs regulate mRNA stability in the TLR and IL-1R signaling pathway.

Notably, regnase-1 protein destabilized regnase-1 mRNA through its 3′ UTR. We identified an evolutionally conserved sequence element in regnase-1 transcript and found that this element can form a stem-loop structure. Disruption of the stem-loop structure abrogated regnase-1-mediated destabilization of mRNA. The regnase-1 target sequence found in IL-6 mRNA 3′ UTR is also reported to form a stem-loop structure. Thus, the stem-loop structure may be the target of regnase-1 for degradation, although further structural studies are required. IκBα mRNA is a target of NF-κB, and IKK-mediated degradation of IκBα leads to synthesis of IκBα protein, which suppresses inflammation. In this context, the self-feedback system can be a common mechanism for suppressing excess inflammation in the recovery phase of infection, as shown in our mathematical model.

A single domain in regnase-1 has dual RNase and deubiquitinase enzymatic functions, and regnase-1 negatively regulates Jnk and NF-κB signaling pathways[34]. In contrast, NF-κB activation in response to LPS is similar in wild-type and regnase-1-deficient macrophages[22], which indicates that regnase-1 is dispensable for the control of NF-κB signaling. We do not have an explanation for this discrepancy in the biological functions of regnase-1. As for the biochemical function of regnase-1, although it is theoretically possible for a single domain to function as both an RNase and a deubiquitinase, a survey of the Enzyme Commission codes for the numerical classification of enzymes among all entries in the UniProt Universal Protein Resource database showed that regnase-1 would be the first such domain of over 12 million entries. Moreover, we were unable to verify the reported homology between regnase-1 and the UCH deubiquitinase domain, for which there is a known structure[34]. On the basis of such preliminary investigations, we expect that further experiments will be needed to clarify the biochemical and biological roles of regnase-1.

The mathematical model qualitatively reproduced the kinetics of the system even after TNF stimulation. There were quantitative differences between the predicted and observed mRNA and protein abundance, however, especially for regnase-1 itself, which suggests that other factors are involved in its regulation. Nevertheless, it would be valuable for future studies of inflammation to translate experimental results into a theoretical framework.

Collectively, our study has demonstrated that IKK activity coupled rapid regulation of transcription and mRNA stability in the course of TLR responses. It is notable that regulators of gene transcription and mRNA stability were reciprocally controlled by a single kinase complex, and mRNA stability must be taken into account to understand the mechanisms of gene regulation in inflammation. These regulatory mechanisms can accomplish both suppression of unwanted inflammation and rapid production of proinflammatory cytokines in response to infection with pathogens.

METHODS

Methods and any associated references are available in the online version of the paper at http://www.nature.com/natureimmunology/.

Note: Supplementary information is available on the Nature Immunology website.

ACKNOWLEDGMENTS

We thank laboratory colleagues; E. Kamada and M. Kageyama for secretarial assistance; Y. Fujiwara, M. Kumagai and N. Umano for technical assistance; M. Takahama and T. Misawa for help with experiments; A. Matsuo, T. Hata, M. Tanaka and T. Kurimoto for discussions; K. Iwai (Osaka University) for expression plasmids for Flag-tagged β-TrCP and β-TrCPΔF; and D.V. Goeddel (Tularik; present affiliation, NGM Biopharmaceuticals) for the expression plasmid for IKKβ; I. Verma and M. Schmitt (Salk Institute), M. Schmidt-Supprian (Max Planck Institute) for MEFs deficient in IKKβ or both IKKα and IKKβ; S. Yamaoka (Tokyo Medical and Dental University) for Rat-1 and 5R cells; and F. Inagaki (Hokkaido University) for recombinant regnase-1 (amino acids 1–330). Supported by the Special Coordination Funds of the Japanese Ministry of Education, Culture, Sports, Science and Technology, and the Ministry of Health, Labour and Welfare in Japan, the Japan Society for the Promotion of Science through Funding Program for World-Leading Innovative R&D on Science and Technology (FIRST Program).

AUTHOR CONTRIBUTIONS

H.I. and O.T. designed and did most of the experiments and analyzed the data; K.M., T.U., K.K., T. Satoh and T. Saitoh helped with experiments; S.T. and D.M.S. did mathematical modeling; M.M. provided advice for experiments; H.I., S.T. and O.T. wrote the manuscript; and S.A. supervised the project.

COMPETING FINANCIAL INTERESTS

The authors declare no competing financial interests.

Published online at http://www.nature.com/natureimmunology/.
Reprints and permissions information is available online at http://www.nature.com/reprints/index.html .

1. Takeuchi, O. & Akira, S. Pattern recognition receptors and inflammation. *Cell* **140**, 805–820 (2010).
2. Beutler, B. Microbe sensing, positive feedback loops, and the pathogenesis of inflammatory diseases. *Immunol. Rev.* **227**, 248–263 (2009).
3. Medzhitov, R. & Horng, T. Transcriptional control of the inflammatory response. *Nat. Rev. Immunol.* **9**, 692–703 (2009).
4. Akira, S., Uematsu, S. & Takeuchi, O. Pathogen recognition and innate immunity. *Cell* **124**, 783–801 (2006).
5. Kawagoe, T. *et al.* Sequential control of Toll-like receptor-dependent responses by IRAK1 and IRAK2. *Nat. Immunol.* **9**, 684–691 (2008).
6. Skaug, B., Jiang, X. & Chen, Z.J. The role of ubiquitin in NF-κB regulatory pathways. *Annu. Rev. Biochem.* **78**, 769–796 (2009).
7. Xia, Z.P. *et al.* Direct activation of protein kinases by unanchored polyubiquitin chains. *Nature* **461**, 114–119 (2009).
8. Gerlach, B. *et al.* Linear ubiquitination prevents inflammation and regulates immune signalling. *Nature* **471**, 591–596 (2011).
9. Ikeda, F. *et al.* SHARPIN forms a linear ubiquitin ligase complex regulating NF-κB activity and apoptosis. *Nature* **471**, 637–641 (2011).
10. Tokunaga, F. *et al.* SHARPIN is a component of the NF-κB-activating linear ubiquitin chain assembly complex. *Nature* **471**, 633–636 (2011).
11. Karin, M. & Ben-Neriah, Y. Phosphorylation meets ubiquitination: the control of NF-κB activity. *Annu. Rev. Immunol.* **18**, 621–663 (2000).
12. Hayden, M.S. & Ghosh, S. Shared principles in NF-κB signaling. *Cell* **132**, 344–362 (2008).
13. Frescas, D. & Pagano, M. Deregulated proteolysis by the F-box proteins SKP2 and β-TrCP: tipping the scales of cancer. *Nat. Rev. Cancer* **8**, 438–449 (2008).
14. Baltimore, D. NF-kappaB is 25. *Nat. Immunol.* **12**, 683–685 (2011).
15. Oeckinghaus, A., Hayden, M.S. & Ghosh, S. Crosstalk in NF-κB signaling pathways. *Nat. Immunol.* **12**, 695–708 (2011).
16. Ea, C.K., Deng, L., Xia, Z.P., Pineda, G. & Chen, Z.J. Activation of IKK by TNFα requires site-specific ubiquitination of RIP1 and polyubiquitin binding by NEMO. *Mol. Cell* **22**, 245–257 (2006).

17. Karin, M. & Gallagher, E. TNFR signaling: ubiquitin-conjugated TRAFfic signals control stop-and-go for MAPK signaling complexes. *Immunol. Rev.* **228**, 225–240 (2009).
18. Anderson, P. Post-transcriptional control of cytokine production. *Nat. Immunol.* **9**, 353–359 (2008).
19. Hao, S. & Baltimore, D. The stability of mRNA influences the temporal order of the induction of genes encoding inflammatory molecules. *Nat. Immunol.* **10**, 281–288 (2009).
20. Anderson, P. Post-transcriptional regulons coordinate the initiation and resolution of inflammation. *Nat. Rev. Immunol.* **10**, 24–35 (2010).
21. Carballo, E., Lai, W.S. & Blackshear, P.J. Feedback inhibition of macrophage tumor necrosis factor-α production by tristetraprolin. *Science* **281**, 1001–1005 (1998).
22. Matsushita, K. *et al.* Zc3h12a is an RNase essential for controlling immune responses by regulating mRNA decay. *Nature* **458**, 1185–1190 (2009).
23. Yamamoto, M. *et al.* Role of adaptor TRIF in the MyD88-independent toll-like receptor signaling pathway. *Science* **301**, 640–643 (2003).
24. Yamaoka, S. *et al.* Complementation cloning of NEMO, a component of the IκB kinase complex essential for NF-κB activation. *Cell* **93**, 1231–1240 (1998).
25. Spencer, E., Jiang, J. & Chen, Z.J. Signal-induced ubiquitination of IκBα by the F-box protein Slimb/β-TrCP. *Genes Dev.* **13**, 284–294 (1999).
26. Hartupee, J., Li, X. & Hamilton, T. Interleukin 1α-induced NFκB activation and chemokine mRNA stabilization diverge at IRAK1. *J. Biol. Chem.* **283**, 15689–15693 (2008).
27. Wan, Y. *et al.* Interleukin-1 receptor-associated kinase 2 is critical for lipopolysaccharide-mediated post-transcriptional control. *J. Biol. Chem.* **284**, 10367–10375 (2009).
28. Kasza, A. *et al.* Transcription factors Elk-1 and SRF are engaged in IL1-dependent regulation of ZC3H12A expression. *BMC Mol. Biol.* **11**, 14 (2010).
29. Paschoud, S. *et al.* Destabilization of interleukin-6 mRNA requires a putative RNA stem-loop structure, an AU-rich element, and the RNA-binding protein AUF1. *Mol. Cell. Biol.* **26**, 8228–8241 (2006).
30. Wu, C.J. & Ashwell, J.D. NEMO recognition of ubiquitinated Bcl10 is required for T cell receptor-mediated NF-κB activation. *Proc. Natl. Acad. Sci. USA* **105**, 3023–3028 (2008).
31. Suzuki, K. & Verma, I.M. Phosphorylation of SNAP-23 by IκB kinase 2 regulates mast cell degranulation. *Cell* **134**, 485–495 (2008).
32. Xia, Y. *et al.* Phosphorylation of p53 by IκB kinase 2 promotes its degradation by β-TrCP. *Proc. Natl. Acad. Sci. USA* **106**, 2629–2634 (2009).
33. Hoshino, K. *et al.* IκB kinase-α is critical for interferon-α production induced by Toll-like receptors 7 and 9. *Nature* **440**, 949–953 (2006).
34. Liang, J. *et al.* MCP-induced protein 1 deubiquitinates TRAF proteins and negatively regulates JNK and NF-κB signaling. *J. Exp. Med.* **207**, 2959–2973 (2010).
35. Hoops, S. *et al.* COPASI—a COmplex PAthway SImulator. *Bioinformatics* **22**, 3067–3074 (2006).

ONLINE METHODS

Mice and reagents. Mice deficient in regnase-1, MyD88 or TRIF have been described[22,23]. All animal experiments were done with the approval of the Animal Research Committee of the Research Institute for Microbial Diseases, Osaka University. LPS from *Salmonella minnesota* was from Invivogen; MALP-2, poly(I:C), R-848 and CpG DNA have been described[22]. Recombinant cytokines were from R&D Systems. Actinomycin D was from Sigma; cycloheximide, MG-132, SB203580, PD98059, SP600125 and LY294002 were from Calbiochem; and TPCA was from TOCRIS.

Cell culture and transfection. Primary MEFs were prepared from wild-type and regnase-1-deficient mouse embryos at embryonic day 13.5. MEFs deficient in IKKα or IKKβ or both IKKα and IKKβ were provided by I. Verma, M. Schmitt and M. Schmidt-Supprian[36,37]. Rat-1 and 5R cells have been described[38]. MEFs, HeLa cells and HEK293 cells were maintained in DMEM (Nacalai Tesque) supplemented with 10% (vol/vol) FBS. Peritoneal exudate cells were prepared from mice 3 d after intraperitoneal injection of 4% (vol/vol) thioglycollate medium (2 ml) and were maintained in RPMI-1640 medium (Nacali Tesque) supplemented with 10% (vol/vol) FBS and 50 μM β-mercaptoethanol. Cells were transfected through the use of Lipofectamine 2000 (Invitrogen), Fugene 6 (Roche) or the Nucleofector system (Lonza).

Construction of plasmids. Regnase-1 (*Zc3h12a*) cDNA has been described[22]. Point mutations of the gene encoding regnase-1 (encoding the substitutions S435A, S439A and S435A,S439A) were made with QuickChange II Site-Directed Mutagenesis Kit (Agilent Technologies). The cDNA was ligated to the vector pFlag-CMV2 (Invitrogen), pcDNA3.1(+)-Myc for expression, pMRX-ires-puro or pMRX-ires-puro-Flag for retrovirus production or pGEX-6P1 (GE Healthcare) for protein production. The 3′ UTR of mouse regnase-1 mRNA was amplified by PCR from mouse genomic DNA and ligated to the plasmid pGL3 (Promega). The plasmids for Flag-tagged IRAK1 and hemagglutinin-tagged ubiquitin have been described[39,40]. Expression plasmids for Flag-tagged β-TrCP or β-TrCP(ΔF) were provided by K. Iwai and the expression plasmid for IKKβ was provided by D.V. Goeddel.

Immunoblot analysis. Whole-cell extracts were prepared in lysis buffer (1% (vol/vol) Nonidet P-40, 150 mM NaCl, 20 mM Tris-HCl, pH 7.5 and 1 mM EDTA supplemented with Complete Mini Protease Inhibitor Cocktail (Roche)). Polyclonal rabbit antibody to regnase-1 was raised against recombinant mouse regnase-1 (amino acids 1–330). The following antibodies were used for immunoblot analysis: antibody to IκBα (anti-IκBα; 9247; Cell Signaling Technology), antibody to phosphorylated IKKα,IKKβ (2697; Cell Signaling Technology), anti-IKKβ (40907; Active Motif), anti-IRAK2 (3595; ProSci), anti-β-actin (C-11; Santa Cruz), anti-c-Myc (C3956 or M4439; Sigma), anti-hemagglutinin (3724; Cell Signaling Technology), anti-Flag (M2 (A8592); Sigma) and anti-ubiquitin (P4D1; Santa Cruz). Rabbit anti-IRAK1 and rabbit anti-IRAK4 have been described[5]. Luminescence was detected with a luminescent image analyzer (ImageQuant LAS 4000).

Treatment with λ-phosphatase and immunoblot analysis. Cell lysates were incubated for 30 min at 30 °C with λ-phosphatase (New England Biolabs), then samples were separated by SDS-PAGE and analyzed by immunoblot.

Immunoprecipitation. HEK293 cells or HeLa cells seeded on 60- or 100-mm dishes were transiently transfected with a total of 1–2 μg of the appropriate combination of plasmids. At 24 h after transfection, cells were lysed in lysis buffer (described above). Proteins were immunoprecipitated from lysates overnight with the appropriate antibodies and protein G Sepharose 4 Fast Flow (GE Healthcare) in lysis buffer. Immune complexes were washed three times with lysis buffer and suspended in SDS sample buffer (lysis buffer containing 3 mM Tris-HCl, pH 6.8, 2% (wt/vol) SDS, 5% (vol/vol) β-mercaptoethanol, 10% (vol/vol) glycerol and bromophenol blue). Samples were boiled for 5 min at 98 °C and separated by SDS-PAGE.

Ubiquitination assay. HeLa cells were incubated for 60 min with MG-132 (1 μM) before stimulation. Transfected HEK293 cells were incubated for 9 h with MG-132 (1 μM) before collection. Cell lysates were boiled for 5 min at 90 °C in 1% (wt/vol) SDS for removal of noncovalently attached proteins, followed by immunoprecipitation with anti-regnase-1 and protein G Sepharose 4 Fast Flow (GE Healthcare) in 0.1% (wt/vol) SDS lysis buffer in the presence of protease inhibitors and MG132 (1 μM). Ubiquitin was detected by immunoblot analysis.

***In vitro* kinase assay.** IKK and IRAK1 *in vitro* kinase assays were done as described[31]. Recombinant IKKα, IKKβ and IRAK1 proteins were from Millipore. GST fusion proteins of regnase-1 (wild-type S435A, S439A and S435, S439A) and GST fusion peptides corresponding to amino acids 430–441 of wild-type regnase-1 (QECLDSGIGSLE) and its S435A, S439A and S435,S439A mutants were produced from *Escherichia coli* as described[22]. GST-IκBα was from Abcam (ab59981). These proteins were incubated for 30 min at 30 °C with 370 kBq of [γ-^{32}P]ATP in kinase buffer (20 mM HEPES, pH 7.7, 20 mM β-glycerophosphate, 10 mM sodium fluoride, 10 mM $MnCl_2$, 10 mM $MgCl_2$ and 2 mM dithiothreitol). Kinase reactions were stopped by heating of the SDS sample buffer, and proteins were separated by SDS-PAGE, then radiolabeled proteins were visualized autoradiography. Total proteins were visualized by staining with Coomassie Brilliant Blue.

Quantitative PCR analysis. TRIzol (Invitrogen) or ZR RNA MicroPrep (Zymo research) was used for the isolation of total RNA, and ReverTra Ace was used according to the manufacturer's instructions (Toyobo) for reverse transcription. For quantitative PCR, DNA fragments were amplified through the use of Thunderbird Probe qPCR Mix (Toyobo) or Thunderbird SYBR qPCR Mix (Toyobo); TaqMan probes for mouse IL-6, human IL-6, human regnase-1, human IκBα and human ICAM1 were from Applied Biosystems. IL-6 primers (forward, 5′-CCGGAGAGGAGACTTCACAG-3′; reverse, 5′-ACAGTGCATCATCGCTGTTC-3′) and β-actin primers (5′-CT ACGTGGGCGACGAGGCCCAGAG-3′, 5′-GGGTACATGGTGGTGCCA CCAGAC-3′) were used for SYBR Green assays. Fluorescence was detected with a StepOne Real-Time PCR System (Applied Biosystems). For analysis of the induction mRNA in response to various stimuli, the abundance of mRNA of each expressed gene was normalized to that of 18S rRNA or β-actin.

Stability of mRNA. Actinomycin D (5 or 10 μg/ml; Sigma) was added directly to cell cultures previously treated with TNF, IL-1β or LPS without removal of the stimulant. Cells were incubated for the appropriate time after the addition of actinomycin D, followed by quantitative PCR analysis of mRNA as described above.

Retroviral transduction of bone marrow–derived macrophages. Bone marrow cells were isolated from regnase-1-deficient mice that had been injected with 5 mg 5-fluorouracil (Nacalai Tesque) intraperitoneally 4 d before preparation. Cells were cultured in stem cell medium (RPMI medium supplemented with 15% (vol/vol) FBS, 10 mM sodium pyruvate, 2 μM L-glutamine, 50 μM β-mercaptoethanol, 100 U/ml of penicillin, 100 U/ml of streptomycin, 100 ng/ml of stem cell factor, 10 ng/ml of IL-6 and 10 ng/ml of IL-3). Then, 48 h later, cells were transduced with retroviral supernatant (supplemented with stem cell factor, IL-6, IL-3 and 10 ng/ml of polybrene) on 2 successive days. Virus was produced by PlatE packaging cells transfected with various plasmids. After the second transduction, cells were washed and resuspended in macrophage growth medium (RPMI-1640 medium supplemented with 10% (vol/vol) FBS, 50 μM β-mercaptoethanol, 100 U/ml of penicillin, 100 μg/ml of streptomycin and 20 ng/ml of macrophage colony-stimulating factor). After 5 d, cells were washed once and cultivated for 2 d with macrophage growth medium plus puromycin (2.5 μg/ml; InvivoGen), then cells were collected for further analysis.

Retroviral transduction of regnase-1-deficient MEFs. MEFs were cultured in DMEM with 10% (vol/vol) FBS, then were transduced with retroviral supernatant on 2 successive days. Virus was produced by PlatE packaging cells transfected with various plasmids. After transduction, cells were washed and resuspended for 24 h in DMEM with 10% (vol/vol) FBS. Cells were washed once and cultured for 36 h in DMEM with puromycin (2 μg/ml; InvivoGen), then stimulated for the appropriate time with IL-1β and collected for further analysis.

doi:10.1038/ni.2137

Tet-off system. HEK293 Tet-off cells (3×10^6) were transfected with pTRE tight plasmid containing sequence encoding a tetracycline-response element plus the β-globin coding sequence and the 3′ UTR of β-globin or regnase-1, together with expression plasmids for wild-type or mutant regnase-1 or control (empty) plasmid. After 3 h, cells were subdivided into three 60-mm dishes and cultured overnight. The transcription of mRNA from pTRE tight vectors was terminated by the addition of doxycycline (1 μg/ml), and total RNA was prepared at the appropriate time. RNA was assessed by RNA-hybridization analysis for measurement of the abundance of β-globin and β-actin mRNA.

Luciferase assay. HEK293 cells were transfected with luciferase reporter plasmid pGL3 containing the 3′ UTR of regnase-1 or empty plasmid together with expression plasmid for regnase-1 or empty control plasmid. After 48 h of cultivation, cells were lysed and luciferase activity in lysates was determined with the Dual-Luciferase Reporter Assay system (Promega). The gene encoding renilla luciferase was transfected simultaneously as an internal control.

Statistical analysis. Statistical significance was calculated with the two-tailed Student's *t*-test. *P* values of less than 0.05 were considered significant.

Additional methods. Information on mathematical modeling (including **Supplementary Fig. 15**) is available in the **Supplementary Methods**.

36. Li, Q., Estepa, G., Memet, S., Israel, A. & Verma, I.M. Complete lack of NF-κB activity in IKK1 and IKK2 double-deficient mice: additional defect in neurulation. *Genes Dev.* **14**, 1729–1733 (2000).
37. Schmidt-Supprian, M. *et al.* Mature T cells depend on signaling through the IKK complex. *Immunity* **19**, 377–389 (2003).
38. Yamamoto, M. *et al.* Key function for the Ubc13 E2 ubiquitin-conjugating enzyme in immune receptor signaling. *Nat. Immunol.* **7**, 962–970 (2006).
39. Uematsu, S. *et al.* Interleukin-1 receptor-associated kinase-1 plays an essential role for Toll-like receptor (TLR)7- and TLR9-mediated interferon-α induction. *J. Exp. Med.* **201**, 915–923 (2005).
40. Tsuchida, T. *et al.* The ubiquitin ligase TRIM56 regulates innate immune responses to intracellular double-stranded DNA. *Immunity* **33**, 765–776 (2010).

doi:10.1038/ni.2137

Immunity
Article

Antiviral Protein Viperin Promotes Toll-like Receptor 7- and Toll-like Receptor 9-Mediated Type I Interferon Production in Plasmacytoid Dendritic Cells

Tatsuya Saitoh,[1,2] Takashi Satoh,[1,2] Naoki Yamamoto,[3] Satoshi Uematsu,[1,2] Osamu Takeuchi,[1,2] Taro Kawai,[1,2] and Shizuo Akira[1,2,*]

[1]Laboratory of Host Defense, WPI Immunology Frontier Research Center, Osaka University, 3-1 Yamada-oka, Suita, Osaka 565-0871, Japan
[2]Department of Host Defense, Research Institute for Microbial Diseases, Osaka University, 3-1 Yamada-oka, Suita, Osaka 565-0871, Japan
[3]Department of Microbiology, Yong Loo Lin School of Medicine, National University of Singapore, Block MD4A, 5 Science Drive 2, 117597, Singapore
*Correspondence: sakira@biken.osaka-u.ac.jp
DOI 10.1016/j.immuni.2011.03.010

SUMMARY

Toll-like receptor 7 (TLR7) and TLR9 sense viral nucleic acids and induce production of type I interferon (IFN) by plasmacytoid dendritic cells (pDCs) to protect the host from virus infection. We showed that the IFN-inducible antiviral protein Viperin promoted TLR7- and TLR9-mediated production of type I IFN by pDCs. Viperin expression was potently induced after TLR7 or TLR9 stimulation and Viperin localized to the cytoplasmic lipid-enriched compartments, lipid bodies, in pDCs. Viperin interacted with the signal mediators IRAK1 and TRAF6 to recruit them to the lipid bodies and facilitated K63-linked ubiquitination of IRAK1 to induce the nuclear translocation of transcription factor IRF7. Loss of Viperin reduced TLR7- and TLR9-mediated production of type I IFN by pDCs. However, Viperin was dispensable for the production of type I IFN induced by intracellular nucleic acids. Thus, Viperin mediates its antiviral function via the regulation of the TLR7 and TLR9-IRAK1 signaling axis in pDCs.

INTRODUCTION

Innate immunity, the first line of host defense against infectious agents, is initiated after the recognition of components of pathogens by pattern-recognition receptors (PRRs) (Medzhitov, 2009; O'Neill and Bowie, 2010; Takeuchi and Akira, 2010). PRRs, such as the Toll-like receptor (TLR), RIG-I-like receptor (RLR), NOD-like receptor (NLR), and the C-type lectin family, drive the coordinated activation of signaling pathways to produce type I interferon (IFN), proinflammatory cytokines, and chemokines, resulting in the induction of host defense response (Medzhitov, 2009; O'Neill and Bowie, 2010; Takeuchi and Akira, 2010).

Production of type I IFN is induced after the detection of viral nucleic acids by PRRs and plays a central role in the establishment of an antiviral state (Medzhitov, 2009; O'Neill and Bowie, 2010; Takeuchi and Akira, 2010). RNA helicases RIG-I and MDA-5, known as RLRs, sense RNA of RNA viruses in the cytoplasm and activate transcription factors IRF3 and IRF7, which induce interferon stimulation responsive element-dependent transcription, resulting in the production of type I IFN (Yoneyama and Fujita, 2010). In contrast, stimulator of interferon genes (STING; also known as MPYS, MITA, or ERIS) mediate the activation of the IRF3-dependent innate immune response induced by a cyclic diadenosine monophosphate of *Listeria monocytogenes* and a double stranded (ds) DNA of DNA viruses (Ishikawa et al., 2009). The IRF3- and IRF7-dependent innate immune responses are also induced after TLR stimulation (Medzhitov, 2009; O'Neill and Bowie, 2010; Takeuchi and Akira, 2010). TLR3 and TLR4 induce IRF3- and IRF7-dependent production of type I IFN after the recognition of extracellular dsRNA and lipopolysaccharide (LPS), respectively (Kawai and Akira, 2010). Plasmacytoid dendritic cells (pDCs) produce a burst amount of type I IFN after the engagement of TLR7 and TLR9. TLR7 detects the single stranded (ss) RNA of RNA viruses and TLR9 detects unmethylated CpG DNA of DNA viruses (Blasius and Beutler, 2010). In pDCs, the engagement of TLR7 or TLR9 in lysosomes triggers the potent activation of IRF7 via kinases IRAK1 and IKKα, leading to the robust production of type I IFN (Blasius and Beutler, 2010).

Inflammatory cytokines and chemokines are also required for the host defense response (Medzhitov, 2009; O'Neill and Bowie, 2010; Takeuchi and Akira, 2010). The engagement of all TLR members and NOD1 and NOD2 triggers the production of proinflammatory cytokines and chemokines via the activation of the transcription factor NF-κB (Medzhitov, 2009; O'Neill and Bowie, 2010; Takeuchi and Akira, 2010). C-type lectins, such as Dectin-1, also mediate the production of inflammatory cytokines via the tyrosine kinase Syk-dependent pathway (Takeuchi and Akira, 2010). Inflammasomes, the caspase-1 containing complexes, induce the processing of pro-IL-1β and subsequent production of the inflammatory cytokine IL-1β after microbial infection (Schroder and Tschopp, 2010). The three types of recognized inflammasomes are: the AIM2 (absent in melanoma 2) inflammasome, activated by cytosolic microbial dsDNA; IPAF (Ice protease-activating factor), activated by bacterial flagellin; and NALP3 (NACHT, LRR, and PYD domains-containing protein 3), activated after damage in an organelle such as disrupted homeostasis of the Golgi apparatus by the M2 protein of influenza virus (Schroder and Tschopp, 2010; Ichinohe et al., 2010).

The IFN-inducible genes, which are upregulated after stimulation by IFNs and the engagement of PRRs, are critically involved in the host defense response against infectious agents (Honda et al., 2006). Targeted disruption of IRF3 and IRF7 and type I IFN receptors renders the host susceptible to viral infection, clearly indicating the importance of type I IFN in antiviral innate immunity (Honda et al., 2006). Although the mechanism underlying the direct elimination of viruses by IFN-inducible genes has been studied for some time, there are still IFN-inducible genes of unknown function in PRR-triggered signaling pathways. Therefore, clarification of the roles of IFN-inducible genes in the regulation of PRR-mediated innate immune responses is clearly important in order to understand host defense.

In the present study we focused on Viperin (also known as RSAD2, Vig1, or Cig5), which was originally identified as one of the inducible genes during infection with human cytomegalovirus (Chin and Cresswell, 2001). Viperin is also induced by type I IFN, type II IFN, LPS, and RNA viruses (Chin and Cresswell, 2001; Severa et al., 2006). Viperin localizes on the endoplasmic reticulum and Golgi apparatus and is transported to lipid-enriched compartments called lipid droplets (Chin and Cresswell, 2001; Hinson and Cresswell, 2009a; Hinson and Cresswell, 2009b). Viperin harbors an amphipathic α-helix domain at its N-terminus and functions by anchoring on a lipid layer via this domain (Hinson and Cresswell, 2009b). Viperin suppresses the replication of influenza virus by disrupting the lipid rafts (Wang et al., 2007). Viperin can also suppress the replication of other types of viruses probably by acting as a radical S-adenosylmethionine (SAM) enzyme (Jiang et al., 2008; Jiang et al., 2010; Duschene and Broderick, 2010; Shaveta et al., 2010). Recentstudies have revealed that Viperin is involved in the activation of NF-κB and AP-1 in T cells (Qiu et al., 2009). However, it is unknown whether Viperin is involved in the PRR-mediated innate immune response. Here, we examined the potential involvement of Viperin in PRR-induced production of type I IFN, inflammatory cytokines, and chemokines and showed Viperin is important in TLR7- and TLR9-mediated production of type I IFN by pDCs.

RESULTS

Viperin Expression Induced by Pathogens

We examined the expression of Viperin after the engagement of various types of PRRs. The engagement of TLR3 and that of TLR4 resulted in the induction of Viperin in peritoneal macrophages (Figure 1A). The engagement of TLR7 and that of TLR9 also resulted in the induction of Viperin in splenic pDCs (Figure 1B). However, ligands for TLR2 or TLR5 failed to trigger the induction of Viperin (Figure 1A). Curdlan and zymosan, ligands for C-type lectin Dectin-1, also failed to induce the expression of Viperin (Figure 1A). The activation of RLR- or STING-signaling pathway resulted in the induction of Viperin in GMCSF-induced DCs (Figures 1C and 1D). The expression of Viperin was also induced after infection by *Salmonella typhimurium*, which triggered both TLR- and NLR-dependent signals (Figure 1D). We examined whether the induction of Viperin was regulated by IRF3 and a related transcription factor IRF7 because IRF3 is able to induce the transcription of Viperin, and these transcription factors are activated by nucleic acids and LPS (Severa et al., 2006; Ishikawa et al., 2009; Kawai and Akira 2010; Yoneyama and Fujita, 2010). Upregulation of Viperin by the pathogens was disrupted in macrophages or GMCSF-induced DCs lacking both IRF3 and IRF7. (Figures 1A, 1C, and 1D). In pDCs, IRF7 is required for TLR7 and TLR9-mediated expression of Viperin (Figure 1B). These results indicated that various types of PRRs could trigger the induction of Viperin via the activation of IRF3 and IRF7 and suggested a potential involvement of Viperin in the regulation of the PRR-mediated innate immune response.

Viperin Facilitates TLR7/9-Dependent Production of Type I IFN

To investigate a role for Viperin in the PRR-mediated innate immune response, we generated Viperin-deficient (*Rsad2*$^{-/-}$) mice (Figure S1A available online). Successful targeted disruption of the Viperin gene locus was confirmed by Southern blotting analysis (Figure S1B). Neither Viperin mRNA nor Viperin protein was detected in *Rsad2*$^{-/-}$ embryonic fibroblasts (Figures S1C and S1D). *Rsad2*$^{-/-}$ mice were found at Mendelian ratios and grew normally (Figure S1E).

We then assessed whether Viperin regulates TLR-dependent production of type I IFN. The production of type I IFN after the engagement of TLR7 with heat-treated Newcastle disease virus (NDV) or TLR9 by CpG DNA was impaired in *Rsad2*$^{-/-}$ FLT3L-induced DCs (Figures 2A and 2B). CpG DNA-induced IFN-β mRNA synthesis was attenuated in *Rsad2*$^{-/-}$ FLT3L-induced DCs, indicating that IFN-β production is reduced at the transcriptional level (Figure 2C). Viperin deficiency reduced the amount of intracellular IFN-α protein in B220^{+} FLT3L-induced DCs (Figure 2D). Consistent with these results, the production of IFN-α induced by A- and D-type CpG DNA was impaired in *Rsad2*$^{-/-}$ splenic pDCs, and the amount of IFN-α in the serum was reduced in *Rsad2*$^{-/-}$ mice injected with A- or D-type CpG DNA (Figures 2E and 2F). These results indicated that Viperin promotes TLR7 and TLR9-dependent production of type I IFN by pDCs. However, Viperin was not involved in the production of IL-12 p40 after TLR7 or TLR9 stimulation, suggesting a selective requirement of Viperin in the TLR7 and TLR9-mediated signaling pathway (Figures 2A–2C, 2E, and 2F). Complementation of wild-type Viperin, but not the N-terminal deletion mutant, into *Rsad2*$^{-/-}$ FLT3L-DCs restored IFN-β production induced by TLR7 or TLR9 engagement (Figure 2G). Because the N terminus of the Viperin protein is an amphipathic α-helix responsible for membrane association, anchoring on the membrane compartments is required for its function in the TLR7- or TLR9-mediated innate immune response. Viperin was dispensable for the TLR4-mediated IFN response because *Rsad2*$^{-/-}$ GMCSF-induced DCs produced normal amounts of IFN-β and CXCL10, an IFN-inducible chemokine, in response to LPS (Figure 2H).

We also assessed the involvement of Viperin in the production of type I IFN induced by intracellular nucleic acids. The production of type I IFN induced by transfected dsRNA or dsDNA was also normal in *Rsad2*$^{-/-}$ MEFs (Figure S2A). Viperin was dispensable for the production of type I IFN induced by NDV, encephalomyocarditis virus (EMCV), *L. monocytogenes*, or herpes simplex virus 1 (HSV1) (Figures S2B and S2C). These results indicated that Viperin does not regulate RLR- and STING-mediated IFN-β production.

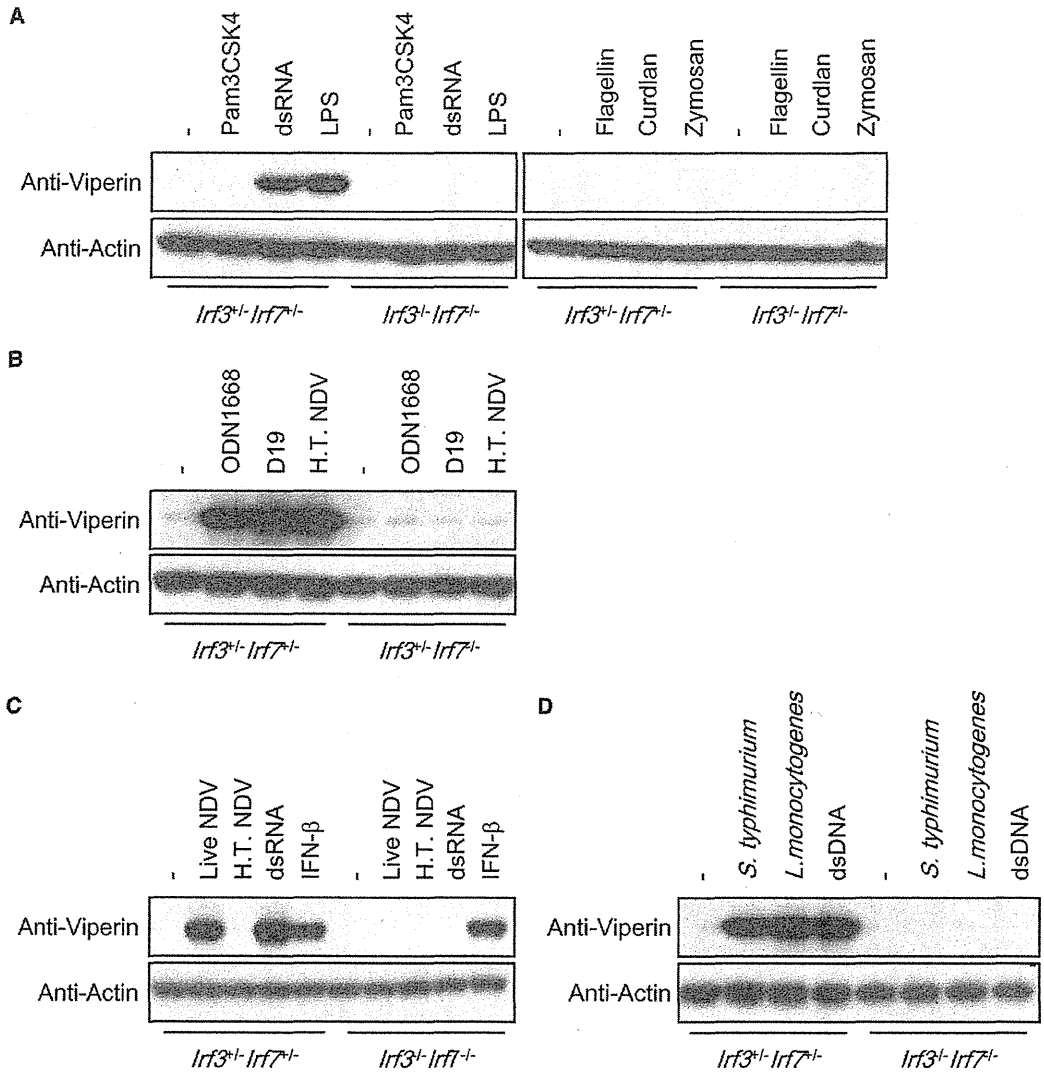

Figure 1. Induction of Viperin after Sensing of Pathogens

(A) Peritoneal macrophages from *Irf3*$^{+/-}$*Irf7*$^{+/-}$ and *Irf3*$^{-/-}$*Irf7*$^{-/-}$ mice were stimulated with the indicated ligands for 5 hr. Whole-cell lysate was subjected to immunoblotting analysis with the indicated antibodies.

(B) Splenic plasmacytoid dendritic cells from *Irf3*$^{+/-}$*Irf7*$^{+/-}$ and *Irf3*$^{+/-}$*Irf7*$^{-/-}$ mice were stimulated with indicated ligands for 5 hr.

(C) GMCSF-induced bone marrow dendritic cells from *Irf3*$^{+/-}$*Irf7*$^{+/-}$ and *Irf3*$^{-/-}$*Irf7*$^{-/-}$ mice were infected with live Newcastle disease virus (NDV) at a multiplicity of infection (MOI) equal to one or heat-treated (H.T.) NDV for 24 hr or were stimulated with dsRNA (poly rI-rC) plus LF2000 or IFN-β for 8 hr.

(D) Peritoneal macrophages from *Irf3*$^{+/-}$*Irf7*$^{+/-}$ and *Irf3*$^{-/-}$*Irf7*$^{-/-}$ mice were infected with *S. typhimurium* (MOI = 0.1) or *L. monocytogenes* (MOI = 20) for 24 hr or were stimulated with dsDNA (poly dA-dT) plus LF2000 for 8 hr. Data are representative of two independent experiments.

We next examined the involvement of Viperin in PRR-induced production of inflammatory cytokines. *Rsad2*$^{-/-}$ macrophages produced a normal amount of TNF and IL-6 after the engagement of TLR2, TLR4, TLR7, or TLR9 (Figure S2D). Viperin was also dispensable for the production of TNF and IL-1β after the engagement of Dectin-1 (Figure S2E). Viperin deficiency did not affect the production of IL-1β by the activation of the AIM2-, IPAF-, or NALP3 inflammasome (Figures S2F and S2G). Viperin was not involved in the enhancement of IL-6 production induced by the engagement of NOD1 or NOD2 (Figure S2H). These results indicated that Viperin does not regulate the production of inflammatory cytokines.

Interaction of Viperin with IRAK1 and TRAF6

Specific involvement of Viperin in TLR7 or TLR9-dependent type I IFN production prompted us to examine the molecular function of Viperin. The population of *Rsad2*$^{-/-}$ B220^{+}CD11C^{+} cells (generally regarded as pDCs; Blasius and Beutler, 2010; Kawai and Akira, 2010) was normal in splenocytes and in FLT3L-induced bone-marrow-derived cells, indicating that Viperin is

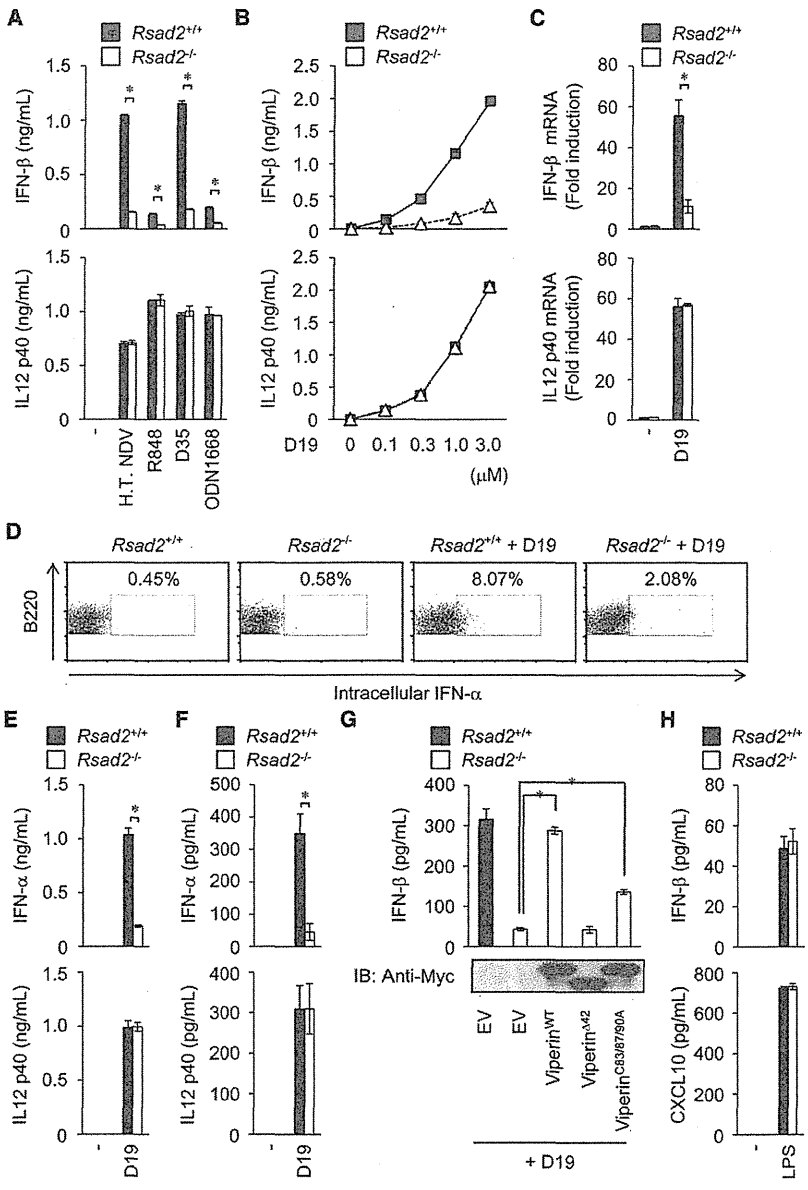

Figure 2. Viperin Promotes TLR7 and TLR9-Dependent Production of Type I IFNs by Plasmacytoid Dendritic Cells

(A and B) *Rsad2*$^{+/+}$ or *Rsad2*$^{-/-}$ FLT3L-induced bone marrow dendritic cells were stimulated with TLR7 ligands (H.T. NDV and R848) or TLR9 ligands (D19, D35 and ODN1668). Culture supernatant was collected 24 hr after stimulation and subjected to ELISA. The results shown are mean ± SD (n = 3). Statistical significance (p value) was determined by the Student's t test. *p < 0.01 (C) *Rsad2*$^{+/+}$ or *Rsad2*$^{-/-}$ FLT3L-induced bone-marrow dendritic cells were stimulated with D19 (1 μM) for 8 hr. Total RNA was isolated and subjected to quantitative RT-PCR analysis for IFN-β and IL-12 p40.

(D) Intracellular IFN-α staining of Flt3L-induced B220^{+} dendritic cells derived from *Rsad2*$^{+/+}$ or *Rsad2*$^{-/-}$ mice. The D19-stimulated cells were stained with anti-B220 and anti-IFN-α and were subjected to flow cytometry analysis.

(E) *Rsad2*$^{+/+}$ or *Rsad2*$^{-/-}$ splenic plasmacytoid dendritic cells were stimulated with D19 for 24 hr.

(F) *Rsad*$^{+/+}$ or *Rsad2*$^{-/-}$ mice were intravenously injected with D19 for the indicated time periods. The collected serum was subjected to ELISA.

(G) Viperin$^{wild\text{-}type}$, Viperin$^{\Delta 42}$, or Viperin$^{C83/87/90A}$ protein was expressed in bone marrow cells isolated from *Rsad2*$^{-/-}$ mice. The transduced cells were cultured in the presence of FLT3L for 7 days and then stimulated with D19 (1 μM) for 24 hr. Culture supernatant and whole-cell lysate were subjected to ELISA and immunoblotting analysis respectively.

(H) *Rsad2*$^{+/+}$ or *Rsad2*$^{-/-}$ GMCSF-induced bone marrow dendritic cells were stimulated with LPS (100 ng/mL) for 24 hr, and the culture supernatant was subjected to ELISA. Data are representative of three independent experiments.

not necessary for the development of pDCs (Figures S3A and S3B). Viperin does not regulate uptake of A- or D-type CpG DNA because the population positive for the FITC-labeled CpG DNA in *Rsad2*$^{-/-}$ B220^{+}CD11C^{+} DCs was comparable to that in wild-type DCs (Figure S3C). The expression level of LC3-I and LCII protein and p62 protein was not altered by Viperin deficiency (Figure S3D), indicating that Viperin does not regulate basal autophagy, which is required for the recognition of the viral genome by TLR7 and TLR9 in pDCs (Lee et al., 2007).

Because Viperin anchors on the cytoplasmic face of a lipid layer of the membrane compartments, we examined whether Viperin regulates essential signal mediators, such as IKKα, IRAK1, IRAK4, IRF7, MyD88, TRAF3, and TRAF6 (Kawai et al., 2004; Honda et al., 2004; Uematsu et al., 2005; Hoshino et al., 2006; Häcker et al., 2006). Viperin is dispensable for A- and D-type CpG DNA-induced phosphorylation of Ser176 and Ser180 residues of IKKα, which is an essential step for IFN response by pDCs (Figure S3E) (Gotoh et al., 2010). In conventional dendritic cells (cDCs), B- and K-type CpG DNA, but not A- and D-type CpG DNA, induces activation of the IKKα-IRF1 signaling axis leading to IFN-β production (Hoshino et al., 2010). Viperin was also dispensable for IKKα-mediated production of IFN-β induced by B- and K-type CpG DNA in cDCs (Figure S3F). These results indicated that Viperin does not regulate the activation of IKKα. We assessed the interaction of Viperin with the remaining essential mediators. When transiently expressed in 293 cells, IRAK1 and TRAF6 interacted with Viperin, whereas the other mediators, IRAK4, IRF7, MyD88, and TRAF3, appeared not to interact with Viperin (Figures 3A and 3B). In FLT3-induced DCs stimulated with A- andD-type CpG DNA, endogenous Viperin interacted with endogenous IRAK1 and endogenous TRAF6 (Figures 3C and 3D). When ectopically expressed, Viperin$^{\Delta 42}$

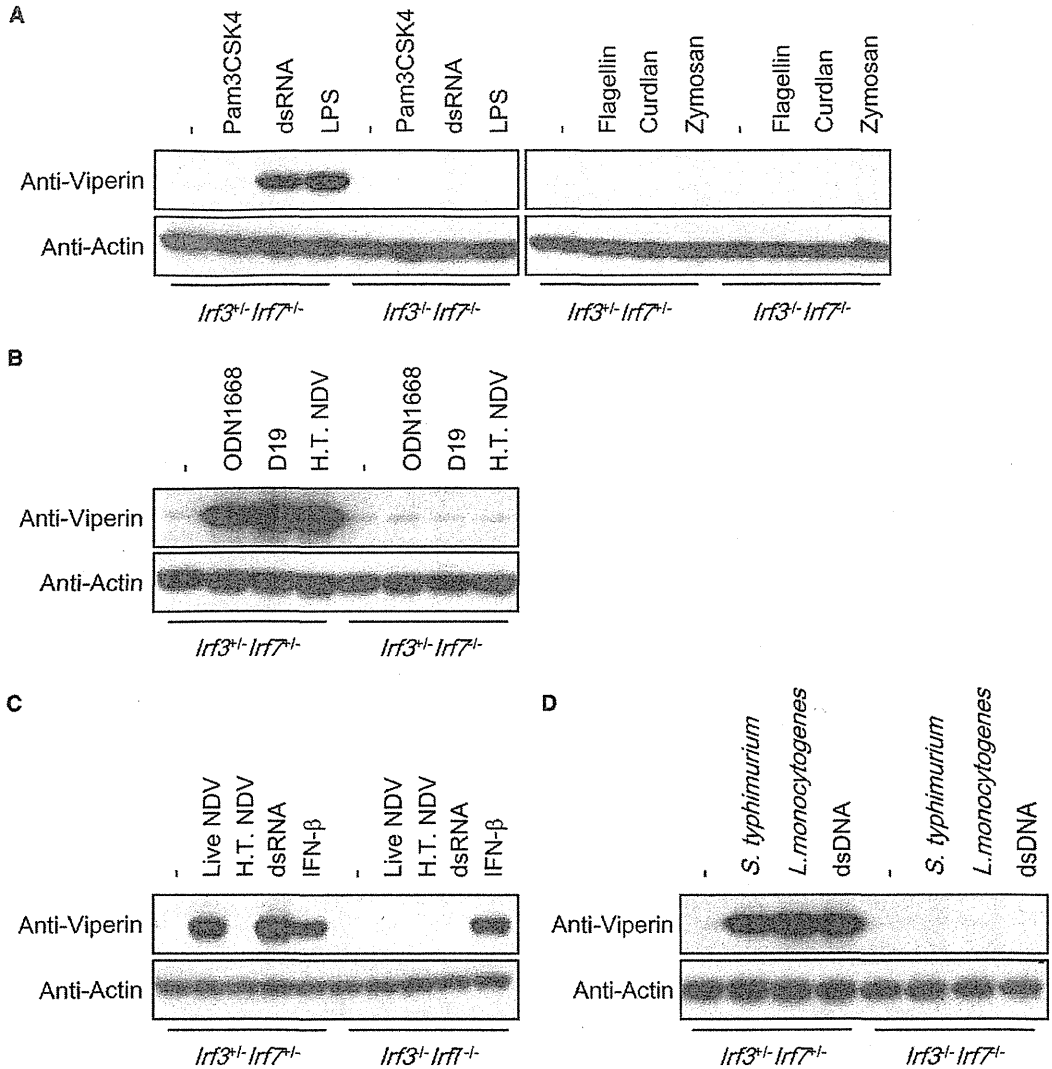

Figure 1. Induction of Viperin after Sensing of Pathogens

(A) Peritoneal macrophages from *Irf3*$^{+/-}$*Irf7*$^{+/-}$ and *Irf3*$^{-/-}$*Irf7*$^{-/-}$ mice were stimulated with the indicated ligands for 5 hr. Whole-cell lysate was subjected to immunoblotting analysis with the indicated antibodies.

(B) Splenic plasmacytoid dendritic cells from *Irf3*$^{+/-}$*Irf7*$^{+/-}$ and *Irf3*$^{+/-}$*Irf7*$^{-/-}$ mice were stimulated with indicated ligands for 5 hr.

(C) GMCSF-induced bone marrow dendritic cells from *Irf3*$^{+/-}$*Irf7*$^{+/-}$ and *Irf3*$^{-/-}$*Irf7*$^{-/-}$ mice were infected with live Newcastle disease virus (NDV) at a multiplicity of infection (MOI) equal to one or heat-treated (H.T.) NDV for 24 hr or were stimulated with dsRNA (poly rI-rC) plus LF2000 or IFN-β for 8 hr.

(D) Peritoneal macrophages from *Irf3*$^{+/-}$*Irf7*$^{+/-}$ and *Irf3*$^{-/-}$*Irf7*$^{-/-}$ mice were infected with *S. typhimurium* (MOI = 0.1) or *L. monocytogenes* (MOI = 20) for 24 hr or were stimulated with dsDNA (poly dA-dT) plus LF2000 for 8 hr. Data are representative of two independent experiments.

We next examined the involvement of Viperin in PRR-induced production of inflammatory cytokines. *Rsad2*$^{-/-}$ macrophages produced a normal amount of TNF and IL-6 after the engagement of TLR2, TLR4, TLR7, or TLR9 (Figure S2D). Viperin was also dispensable for the production of TNF and IL-1β after the engagement of Dectin-1 (Figure S2E). Viperin deficiency did not affect the production of IL-1β by the activation of the AIM2-, IPAF-, or NALP3 inflammasome (Figures S2F and S2G). Viperin was not involved in the enhancement of IL-6 production induced by the engagement of NOD1 or NOD2 (Figure S2H). These results indicated that Viperin does not regulate the production of inflammatory cytokines.

Interaction of Viperin with IRAK1 and TRAF6

Specific involvement of Viperin in TLR7 or TLR9-dependent type I IFN production prompted us to examine the molecular function of Viperin. The population of *Rsad2*$^{-/-}$ B220^{+}CD11C^{+} cells (generally regarded as pDCs; Blasius and Beutler, 2010; Kawai and Akira, 2010) was normal in splenocytes and in FLT3L-induced bone-marrow-derived cells, indicating that Viperin is

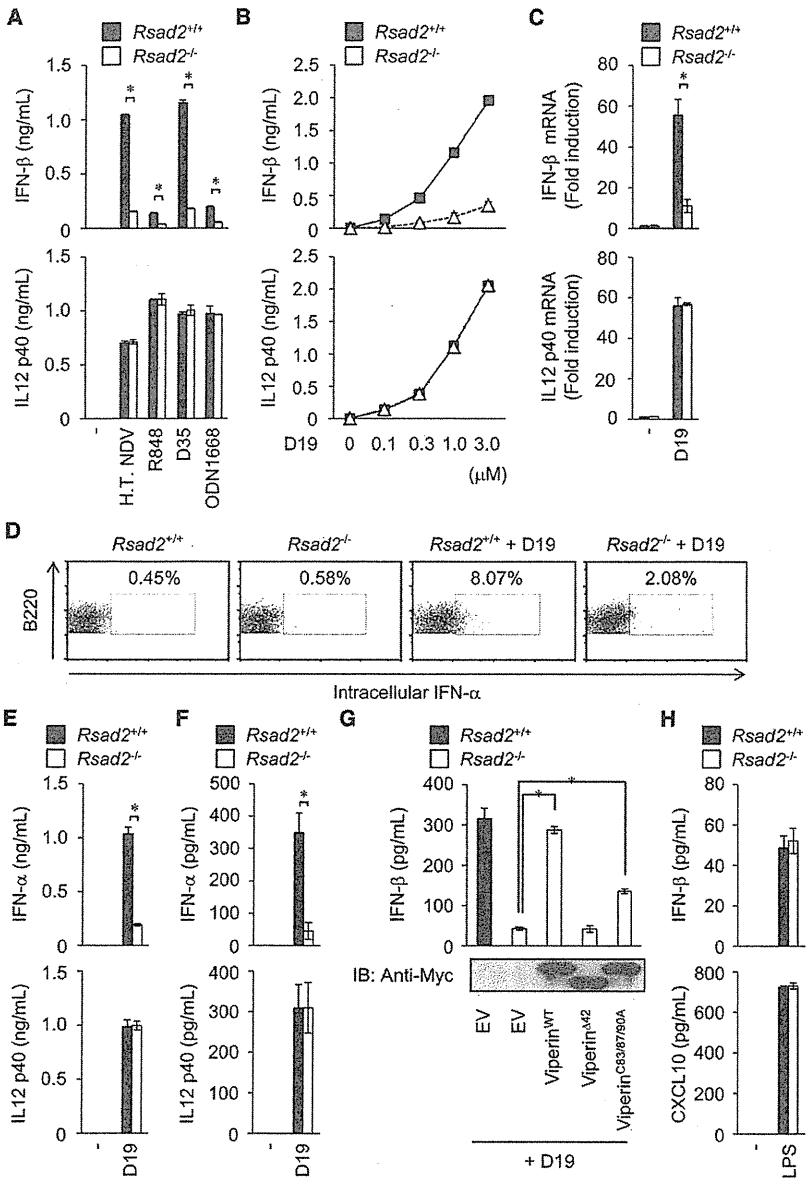

Figure 2. Viperin Promotes TLR7 and TLR9-Dependent Production of Type I IFNs by Plasmacytoid Dendritic Cells

(A and B) *Rsad2*$^{+/+}$ or *Rsad2*$^{-/-}$ FLT3L-induced bone marrow dendritic cells were stimulated with TLR7 ligands (H.T. NDV and R848) or TLR9 ligands (D19, D35 and ODN1668). Culture supernatant was collected 24 hr after stimulation and subjected to ELISA. The results shown are mean ± SD (n = 3). Statistical significance (p value) was determined by the Student's t test. *p < 0.01 (C) *Rsad2*$^{+/+}$ or *Rsad2*$^{-/-}$ FLT3L-induced bone-marrow dendritic cells were stimulated with D19 (1 μM) for 8 hr. Total RNA was isolated and subjected to quantitative RT-PCR analysis for IFN-β and IL-12 p40.

(D) Intracellular IFN-α staining of Flt3L-induced B220^{+} dendritic cells derived from *Rsad2*$^{+/+}$ or *Rsad2*$^{-/-}$ mice. The D19-stimulated cells were stained with anti-B220 and anti-IFN-α and were subjected to flow cytometry analysis.

(E) *Rsad2*$^{+/+}$ or *Rsad2*$^{-/-}$ splenic plasmacytoid dendritic cells were stimulated with D19 for 24 hr.

(F) *Rsad*$^{+/+}$ or *Rsad2*$^{-/-}$ mice were intravenously injected with D19 for the indicated time periods. The collected serum was subjected to ELISA.

(G) Viperin$^{wild\text{-}type}$, Viperin$^{\Delta 42}$, or Viperin$^{C83/87/90A}$ protein was expressed in bone marrow cells isolated from *Rsad2*$^{-/-}$ mice. The transduced cells were cultured in the presence of FLT3L for 7 days and then stimulated with D19 (1 μM) for 24 hr. Culture supernatant and whole-cell lysate were subjected to ELISA and immunoblotting analysis respectively.

(H) *Rsad2*$^{+/+}$ or *Rsad2*$^{-/-}$ GMCSF-induced bone marrow dendritic cells were stimulated with LPS (100 ng/mL) for 24 hr, and the culture supernatant was subjected to ELISA. Data are representative of three independent experiments.

not necessary for the development of pDCs (Figures S3A and S3B). Viperin does not regulate uptake of A- or D-type CpG DNA because the population positive for the FITC-labeled CpG DNA in *Rsad2*$^{-/-}$ B220^{+}CD11C^{+} DCs was comparable to that in wild-type DCs (Figure S3C). The expression level of LC3-I and LCII protein and p62 protein was not altered by Viperin deficiency (Figure S3D), indicating that Viperin does not regulate basal autophagy, which is required for the recognition of the viral genome by TLR7 and TLR9 in pDCs (Lee et al., 2007).

Because Viperin anchors on the cytoplasmic face of a lipid layer of the membrane compartments, we examined whether Viperin regulates essential signal mediators, such as IKKα, IRAK1, IRAK4, IRF7, MyD88, TRAF3, and TRAF6 (Kawai et al., 2004; Honda et al., 2004; Uematsu et al., 2005; Hoshino et al., 2006; Häcker et al., 2006). Viperin is dispensable for A- and D-type CpG DNA-induced phosphorylation of Ser176 and Ser180 residues of IKKα, which is an essential step for IFN response by pDCs (Figure S3E) (Gotoh et al., 2010). In conventional dendritic cells (cDCs), B- and K-type CpG DNA, but not A- and D-type CpG DNA, induces activation of the IKKα-IRF1 signaling axis leading to IFN-β production (Hoshino et al., 2010). Viperin was also dispensable for IKKα-mediated production of IFN-β induced by B- and K-type CpG DNA in cDCs (Figure S3F). These results indicated that Viperin does not regulate the activation of IKKα. We assessed the interaction of Viperin with the remaining essential mediators. When transiently expressed in 293 cells, IRAK1 and TRAF6 interacted with Viperin, whereas the other mediators, IRAK4, IRF7, MyD88, and TRAF3, appeared not to interact with Viperin (Figures 3A and 3B). In FLT3-induced DCs stimulated with A- andD-type CpG DNA, endogenous Viperin interacted with endogenous IRAK1 and endogenous TRAF6 (Figures 3C and 3D). When ectopically expressed, Viperin$^{\Delta 42}$